YANKEE ATOMIC ELECTRIC COMPANY

YAEC-1867

Vermont Yankee
Cycle 17
Core Performance Analysis Report

June 1993

Major Contributors: C. Chiu
B. Hubbard
M. LeFrancois
S. Mihaiu-Westerlind
D. Morin
J. Neyman
A. Robertshaw
J. Robichaud
L. Schor
F. Seifaee
R. P. Smith
K. E. St.John
R. A. Woehlke

Prepared by: M A Sironen 7-27-93
M. A. Sironen (Date)
VY Nuclear Engineering Coordinator

Approved by: R J Cacciapouti 7/27/93
R. J. Cacciapouti, Manager (Date)
Reactor Physics Group

Approved by: P. A. Bergeron 7/28/93
P. A. Bergeron, Manager (Date)
Transient Analysis Group

Approved by: R K Sundaram 7/28/93
R. K. Sundaram, Manager (Date)
LOCA Analysis Group

Approved by: B C Slifer 7/28/93
B. C. Slifer, Director (Date)
Nuclear Engineering Department

Yankee Atomic Electric Company
Nuclear Services Division
580 Main Street
Bolton, Massachusetts 01740

DISCLAIMER OF RESPONSIBILITY

This document was prepared by Yankee Atomic Electric Company ("Yankee"). The use of information contained in this document by anyone other than Yankee, or the Organization for which this document was prepared under contract, is not authorized and, with respect to any unauthorized use, neither Yankee nor its officers, directors, agents, or employees assume any obligation, responsibility, or liability or make any warranty or representation as to the accuracy or completeness of the material contained in this document.

ABSTRACT

This report presents design information, calculational results, and operating limits pertinent to the operation of Cycle 17 of the Vermont Yankee Nuclear Power Station. These include the fuel design and core loading pattern descriptions; calculated reactor power distributions, exposure distributions, shutdown capability, and reactivity data; and the results of safety analyses performed to justify plant operation throughout the cycle.

ACKNOWLEDGEMENTS

The author and major contributors would like to acknowledge the contributions to this work by the Vermont Yankee Reactor & Computer Engineering Department for their review of input data and guidance.

TABLE OF CONTENTS

TABLE OF CONTENTS
(Continued)

LIST OF FIGURES

LIST OF FIGURES
(Continued)

LIST OF TABLES

LIST OF TABLES
(Continued)

1.0 INTRODUCTION

This report provides information to support the operation of the Vermont Yankee Nuclear Power Station through the forthcoming Cycle 17. In this report, Cycle 17 will be referred to as the Reload Cycle. The preceding Cycle 16 will be referred to as the Current Cycle. The Cycle 16/17 refueling will involve the discharge of 128 irradiated fuel bundles and the insertion of 128 new fuel bundles. The resultant core will consist of 128 new fuel bundles and 240 irradiated fuel bundles. The General Electric Company (GE) manufactured all the bundles. Some of the irradiated fuel was also present in the reactor in Cycle 15. This cycle will be referred to as the Past Cycle.

This report contains descriptions and analyses results pertaining to the mechanical, thermal-hydraulic, physics, and safety aspects of the Reload Cycle. The MAPLHGR and MCPR operating limits calculated for the Reload Cycle are given in Appendix A. These limits will be included in the Core Operating Limits Report.

2.0 RECENT REACTOR OPERATING HISTORY

2.1 Operating History of the Current Cycle

The current operating cycle is Cycle 16. To date, the Current Cycle has been operating at, or near, full power with the exception of sequence exchanges, repair to the Motor-Generator sets at 40% power, and one short repair outage. Coastdown is expected to start in late July. The operating history highlights and control rod sequence exchange schedule of the Current Cycle are found in Table 2.1.1.

2.2 Operating History of Past Applicable Cycle

The irradiated fuel in the Reload Cycle includes some fuel bundles initially inserted in Cycle 15. This Past Cycle operated at, or near, full power with the exception of sequence exchanges, one short repair outage, four scrams, and a coastdown to the end of cycle. The operating history highlights of the Past Cycle are found in Table 2.2.1. The Past Cycle is described in detail in the Cycle 15 Summary Report[1].

TABLE 2.1.1

VY CYCLE 16 OPERATING HIGHLIGHTS

Beginning of Cycle Date	April 19, 1992
End of Cycle Date	August 28, 1993*
Weight of Uranium As-Loaded (Short Tons)	72.06
Beginning of Cycle Core Average Exposure** (MWd/St)	11417
End of Full Power Core Average Exposure** (MWd/St)	21187*
End of Cycle Core Average Exposure** (MWd/St)	21863*
Number of Fresh Assemblies	128
Number of Irradiated Assemblies	240

Control Rod Sequence Exchange Schedule:

	Sequence	
Date	From	To
June 14, 1992	A2-1	B2-1
August 9, 1992	B2-1	A1-1
October 15, 1992	A1-1	B1-1
December 7, 1992	B1-1	A2-2
February 9, 1993	A2-2	B2-2
April 6, 1993	B2-2	A1-2
June 6, 1993	A1-2	B1-2

* Projected dates and exposures.

** Exposures based on the Plant Process Computer accounting.

TABLE 2.2.1

VY CYCLE 15 OPERATING HIGHLIGHTS

Beginning of Cycle Date	October 14, 1990
End of Cycle Date	March 7, 1992
Weight of Uranium As-Loaded (Short Tons)	72.95
Beginning of Cycle Core Average Exposure (MWd/St)	10809
End of Full Power Core Average Exposure (MWd/St)	20046
End of Cycle Core Average Exposure (MWd/St)	21082
Number of Fresh Assemblies	128
Number of Irradiated Assemblies	240

Control Rod Sequence Exchange Schedule:

	Sequence	
Date	From	To
December 15, 1990	A2-1	B1-1
January 28, 1991	B1-1	B2-1
March 12, 1991	B2-1	A1-1
May 19, 1991	A1-1	A2-2
July 21, 1991	A2-2	B1-2
September 14, 1991	B1-2	B2-2
November 23, 1991	B2-2	A1-2

3.0 RELOAD CORE DESIGN DESCRIPTION

3.1 Core Fuel Loading

The Reload Cycle core will consist of both new and irradiated assemblies. All the assemblies have bypass flow holes drilled in the lower tie plate. Table 3.1.1 characterizes the core by fuel type, batch size, and first cycle loaded. A description of the fuel is found in the GE Standard Application for Reactor Fuel[2] and the GE Fuel Bundle Design Reports[3][4].

3.2 Design Reference Core Loading Pattern

The Reload Cycle assembly locations are indicated on the map in Figure 3.2.1. For the sake of legibility only the lower right quadrant is shown. The other quadrants are mirror images with bundles of the same type having nearly identical exposures. The bundles are identified by the reload number in which they were first introduced into the core. Table 3.1.1 provides the key, called bundle ID, which identifies what explicit fuel type is found in each bundle location.

If any changes are made to the loading pattern at the time of refueling, they will be evaluated under 10CFR50.59. The final loading pattern with specific fuel bundle serial numbers will be supplied in the Startup Test Report.

3.3 Assembly Exposure Distribution

The assumed nominal exposure on the fuel bundles in the Reload Cycle design reference loading pattern is given in Figure 3.2.1. To obtain this exposure distribution, the Past Cycle was depleted with the SIMULATE-3 model[5],[6] using actual plant operating history. For the Current Cycle, plant operating history was used through December 4, 1992. Beyond this date, the exposure was accumulated using a best-estimate rodded depletion analysis to End of Full Power Life (EOFPL) followed by a projected coastdown to End of Cycle (EOC).

Table 3.3.1 gives the assumed nominal exposure on the Current Cycle and the Beginning of Cycle core average exposure that results from the shuffle into the Reload Cycle loading pattern. The Reload Cycle EOFPL core average exposure and cycle capability are provided.

TABLE 3.1.1

ASSUMED VY CYCLE 17 FUEL BUNDLE TYPES AND NUMBERS

	Fuel Type Designation	Reload Bundle ID	Cycle Loaded	Number of Bundles
Irradiated	BP8DWB311-10GZ	R14A	15	52
	BP8DWB311-11GZ	R14B	15	60
	BP8DWB311-10GZ	R15A	16	40
	BP8DWB311-11GZ	R15B	16	88
New	BP8DWB335-10GZ	R16A	17	96
	BP8DWB335-11GZ	R16B	17	32

TABLE 3.3.1

DESIGN BASIS VY CYCLE 16 AND CYCLE 17 EXPOSURES*

Assumed End of Current Cycle Core Average Exposure with an Exposure Window of ± 600 MWd/St[7]	21.83±.6 GWd/St
Assumed Beginning of Reload Cycle Core Average Exposure	11.49 GWd/St
Haling Calculated End of Full Power Life Reload Cycle Core Average Exposure	21.66 GWd/St
Reload Cycle Full Power Exposure Capability	10.17 CWd/St

* Exposures based on the SIMULATE-3 accounting.

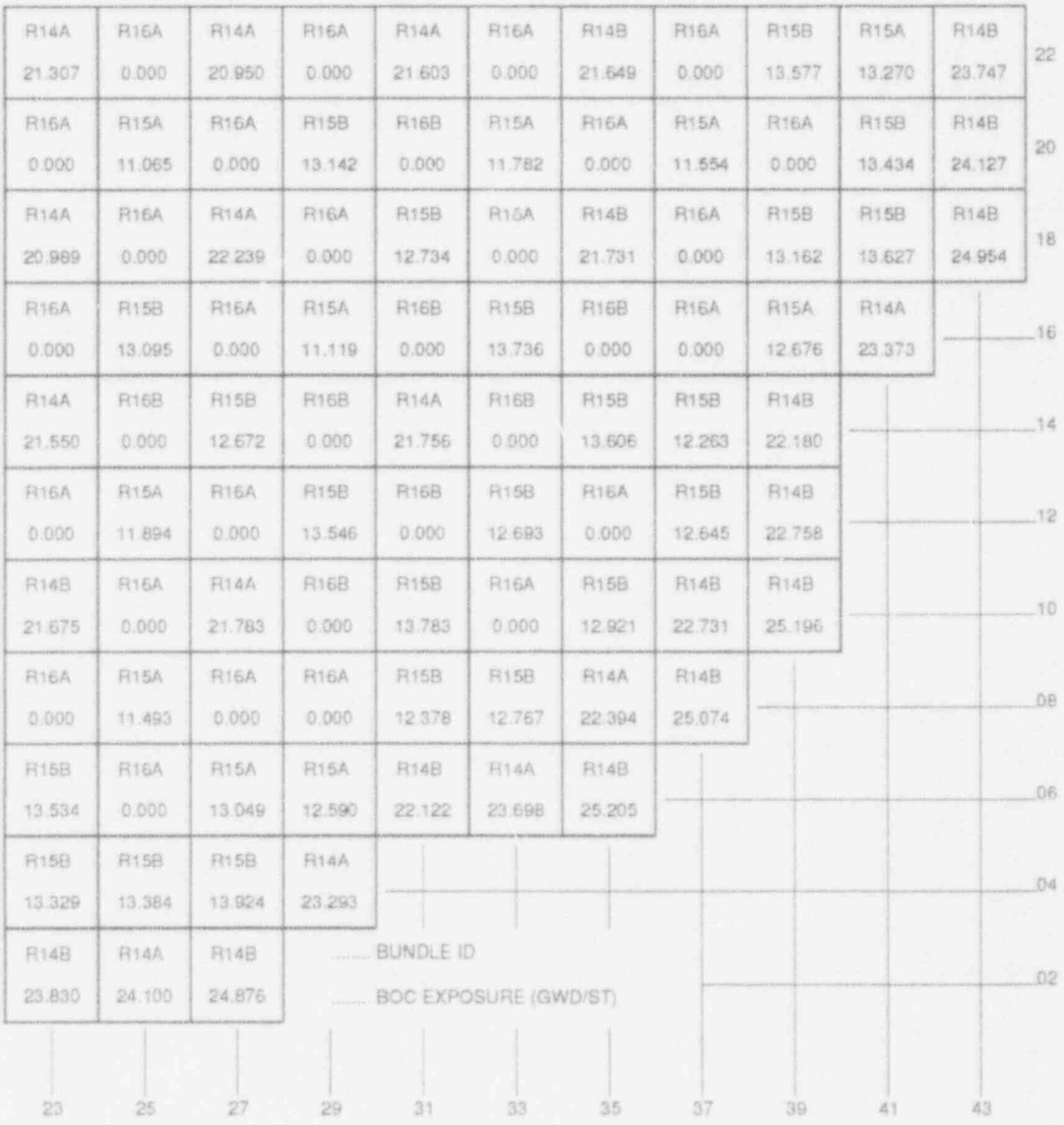

FIGURE 3.2.1

VY CYCLE 17 DESIGN REFERENCE LOADING PATTERN, LOWER RIGHT QUADRANT

4.0 FUEL MECHANICAL AND THERMAL DESIGN

4.1 Mechanical Design

All of the fuel to be inserted into the Reload Cycle was fabricated by GE. The major mechanical design parameters are given in Table 4.1.1 and Reference 2. Detailed descriptions of the fuel rod mechanical design and mechanical design analyses are provided in Reference 2. These design analyses remain valid with respect to the Reload Cycle operation. Mechanical and chemical compatibility of the fuel bundles with the in-service reactor environment is also addressed in Reference 2.

4.2 Thermal Design

The fuel thermal effects calculations were performed using the FROSSTEY-2 computer code[8],[9],[10]. The FROSSTEY-2 code calculates pellet-to-cladding gap conductance and fuel temperatures from a combination of theoretical and empirical models including but not limited to fuel and cladding thermal expansion, fission gas release, pellet swelling, pellet densification, pellet cracking, and fuel and cladding thermal conductivity.

The thermal effects analysis included the calculation of fuel temperatures and pellet-to-cladding gap conductance under core average and hot channel conditions. The core average calculations integrate the responses of individual fuel batch average operating histories over the core average exposure range of the Reload Cycle. These gap conductance values are weighted axially into 12 axial nodes by power distributions and radially by volume. The core-wide gap conductance values for the RETRAN system simulations, described in Sections 7.1 and 7.2, are from this data set at the corresponding exposure statepoints. Table 4.2.1 provides the core average response of gap conductance.

The hot channel gap conductance values, which are input to the hot channel transient calculations (Section 7.1), were evaluated for

the limiting fuel bundle type as a function of the assembly exposure for two axial power shapes, a 1.4 chopped cosine and the Reload Cycle's Haling. The hot channel calculations assumed the following as required by the NRC Safety Evaluation for FROSSTEY-2[11]: 1) appropriate allowances to account for manufacturing uncertainties and 2) the worst axial power shape prior to the transient. The peak power node was placed at the maximum average planar linear heat generation rate (MAPLHGR) limits. Gap conductance values for the hot channel analysis were determined using the limiting bundle exposure. The limiting bundle is defined as the bundle with the lowest MCPR or the highest power, if different, within the exposure range of interest. The limiting exposure for the bundle is defined by the exposure which produces the highest bundle average gap conductance within the interval of interest. The SIMULATE-3 rodded depletion (Section 5.1.2) provided predictions of the limiting bundle exposure for each exposure interval. Table 4.2.2 provides the hot channel gap conductance values for the two axial power shapes. Results are presented for the bounding exposure for the chopped cosine shape and at the four exposure statepoints for the Haling shape.

4.3 Operating Experience

All irradiated fuel bundles scheduled to be reinserted in the Reload Cycle have operated as expected in past cycles of Vermont Yankee. Off-gas measurements in the Current Cycle have indicated a small fuel rod failure. Vermont Yankee is planning to assure that the failed rod(s) are not inserted into the Reload Cycle.

TABLE 4.1.1

NOMINAL FUEL MECHANICAL DESIGN PARAMETERS

Fuel Bundle*	Irradiated Fuel Type	New Fuel Type
Bundle Types	GE8X8NB	GE8X8NB
Vendor Designation	BP8DWB311-10GZ & BP8DWB311-11GZ	BP8DWB335-10GZ & BP8DWB335-11GZ
Initial Enrichment, w/o U_{235}	3.11	3.35
Rod Array	8X8	8X8
Fuel Rods per Bundle	60	60
Outer Fuel Channel		
Material	Zr-2	Zr-2
Wall Thickness, inches	0.080	0.080

* Complete bundle, rod, and pellet descriptions are found in References 2 through 4.

TABLE 4.2.1

VY CYCLE 17 CORE AVERAGE GAP CONDUCTANCE VALUES

Axial Node	Gap Conductance (BTU/hr-ft²-°F)			
	BOC	EOFPL-2000 MWd/St	EOFPL-1000 MWd/St	EOFPL
1	1015	1785	1895	2040
2	2310	3650	3760	3935
3	2475	3915	4020	4380
4	2495	3940	4050	4425
5	2540	3975	4120	4540
6	2700	4090	4390	4890
7	2640	3965	4265	4740
8	2670	4075	4345	4890
9	2360	3615	3735	4105
10	2270	3270	3385	3560
11	1365	2370	2565	2605
12	610	725	745	750

TABLE 4.2.2

VY CYCLE 17 HOT CHANNEL GAP CONDUCTANCE VALUES*

Gap Conductance (BTU/hr-ft^2-°F)

Axial Node	Haling Axial Power Distribution				1.4 Chopped Cosine Power Distribution
	BOC	EOFPL-2000 MWd/St	EOFPL-1000 MWd/St	EOFPL	Bounding Exposure
1	2803	2717	2927	3506	762
2	7436	7669	7664	8545	1446
3	9910	8371	9742	9254	4102
4	10002	9055	9764	9266	7259
5	10001	10035	9764	9268	10110
6	10002	10049	9764	9270	10130
7	9998	10045	9760	9267	10133
8	9998	10045	9760	9267	10133
9	9524	8439	9760	9267	8324
10	7514	7671	7837	8787	6590
11	4597	4259	5081	5657	2419
12	1195	1185	1209	1267	922

* The hot channel gap conductance values are derived for the BP8DWB335 fuel type because it is conservative compared to the other fuel types.

5.0 NUCLEAR DESIGN

5.1 Core Power Distributions

The Reload Cycle was depleted using SIMULATE-3 to give both a rodded depletion and an All Rods Out (ARO) Haling depletion.

5.1.1 Haling Power Distribution

The Haling depletion serves as the basis for defining core reactivity characteristics for most transient evaluations. This is primarily because its flat power shape has conservatively weak scram characteristics. Sensitivity studies have shown that the limiting pressurization transient results are more conservative when calculated using the Haling power distribution as the initial power shape.

The Haling power distribution is calculated in the ARO condition. The Haling iteration converges on a self-consistent power and exposure distribution for the burnup step to EOFPL. In principle, this should provide the overall minimum peaking power shape for the cycle. During the actual cycle, flatter power distributions might occasionally be achieved by shaping with control rods. However, such shaping would leave underburned regions in the core which would peak at another point in time. Figures 5.1.1 and 5.1.2 give the Haling radial and axial average power distributions for the Reload Cycle.

5.1.2 Rodded Depletion Power Distribution

The rodded depletion was used to evaluate the mislocated bundle error and the rod withdrawal error because it provides the initial rod patterns and more accurately defines the local characteristics prior to the transient evaluations. It was also used in the rod drop worth and shutdown margin calculations because it depletes the top of the core more realistically than the Haling depletion. The rodded depletion also provides the hot channel bundle exposures for the gap conductance calculation.

To generate the rodded depletion, control rod patterns were developed which give critical eigenvalues at several points in the cycle and peaking similar to the Haling calculation. The resulting patterns were frequently more peaked than the Haling, but were below expected operating limits. However, as stated above, the underburned regions of the core can exhibit peaking in excess of the Haling peaking when pulling ARO at EOFPL. Figures 5.1.3 and 5.1.4 give the ARO radial and axial average power distributions for the Reload Cycle rodded depletion at EOFPL.

5.2 Core Exposure Distributions

The Reload Cycle exposures are summarized in Table 3.3.1. The projected BOC radial exposure distribution for the Reload Cycle is given in Figure 3.2.1. The Haling calculation produced the EOFPL radial exposure distribution given in Figure 5.2.1. Since the Haling power shape is constant, it can be held fixed by SIMULATE-3 to give the exposure distributions at various mid-cycle points. BOC, EOFPL-2000 MWd/St, EOFPL-1000 MWd/St, and EOFPL exposure distributions were used to develop reactivity input for the core wide transient analyses.

The rodded depletion differs from the Haling during the cycle because the rods shape the power differently. However, rod sequences are swapped frequently and the overall exposure distribution at end of cycle is similar to the Haling. Figure 5.2.2 gives the EOFPL radial exposure distribution for the Reload Cycle rodded depletion.

5.3 Cold Shutdown Margin

Technical Specifications[12] state that, for sufficient shutdown margin, the core must be subcritical by at least 0.25% $\Delta K + R$ (defined below) with the strongest worth control rod withdrawn. Using SIMULATE-3, a search was made for the strongest worth control rod at various exposures in the cycle. This is necessary because rod worths change with exposure on adjacent assemblies. Then the cold K_{eff} with the strongest rod out was calculated at BOC and at the end of each

control rod sequence. Subtracting each cold K_{eff} with the strongest rod out from the cold critical K_{eff} defines the shutdown margin as a function of exposure. Figure 5.3.1 shows the results.

The cold critical K_{eff} was defined as the average calculated critical K_{eff} minus a 95% confidence level uncertainty. Then all cold results were normalized to make the critical K_{eff} equal to 1.000.

Because the local reactivity may increase with exposure, the shutdown margin (SDM) may decrease. To account for this and other uncertainties, the value R is calculated. R is defined as R_1 plus R_2. R_1 is the difference between the cold K_{eff} with the strongest rod out at BOC and the maximum cold K_{eff} with the strongest rod out in the cycle. R_2 is a measurement uncertainty in the demonstration of SDM associated with the manufacture of past control blades. It is presently set at 0.07% ΔK[13],[14]. The shutdown margin results, summarized in Table 5.3.1, show that the shutdown margin for the Reload Cycle is greater than the Technical Specifications limit of 0.32% ΔK.

5.4 Maximum K_∞ for the Spent Fuel Pool

Section 5.5E of the Technical Specifications requires that the K_∞ for any bundle stored in either the new fuel vault or the spent fuel pool not exceed 1.31 to ensure compliance with the K_{eff} safety limit of 0.95. The bundles used in the Reload Cycle do not exceed the specifications in Section 5.5E, as shown in Table 5.4.1. These values are obtained from CASMO-3G[15].

TABLE 5.3.1

VY CYCLE 17 K_{eff} VALUES AND SHUTDOWN MARGIN CALCULATION

Cold Critical K_{eff}	1.0000
BOC K_{eff} - Controlled With Strongest Worth Rod Withdrawn	0.9869
Cycle Minimum Shutdown Margin Occurs at BOC With Strongest Worth Rod Withdrawn	1.31% ΔK
R_1, Maximum Increase in Cold K_{eff} With Exposure	0.00% ΔK

TABLE 5.4.1

VY CYCLE 17 MAXIMUM COLD K_∞ OF ANY ENRICHED SEGMENT

Bundle Type	Maximum K_∞
BP8DWB311-10GZ	1.20
BP8DWB311-11GZ	1.20
BP8DWB335-10GZ	1.22
BP8DWB335-11GZ	1.22

FIGURE 5.1.1

VY CYCLE 17 HALING DEPLETION,
EOFPL BUNDLE AVERAGE RELATIVE POWERS

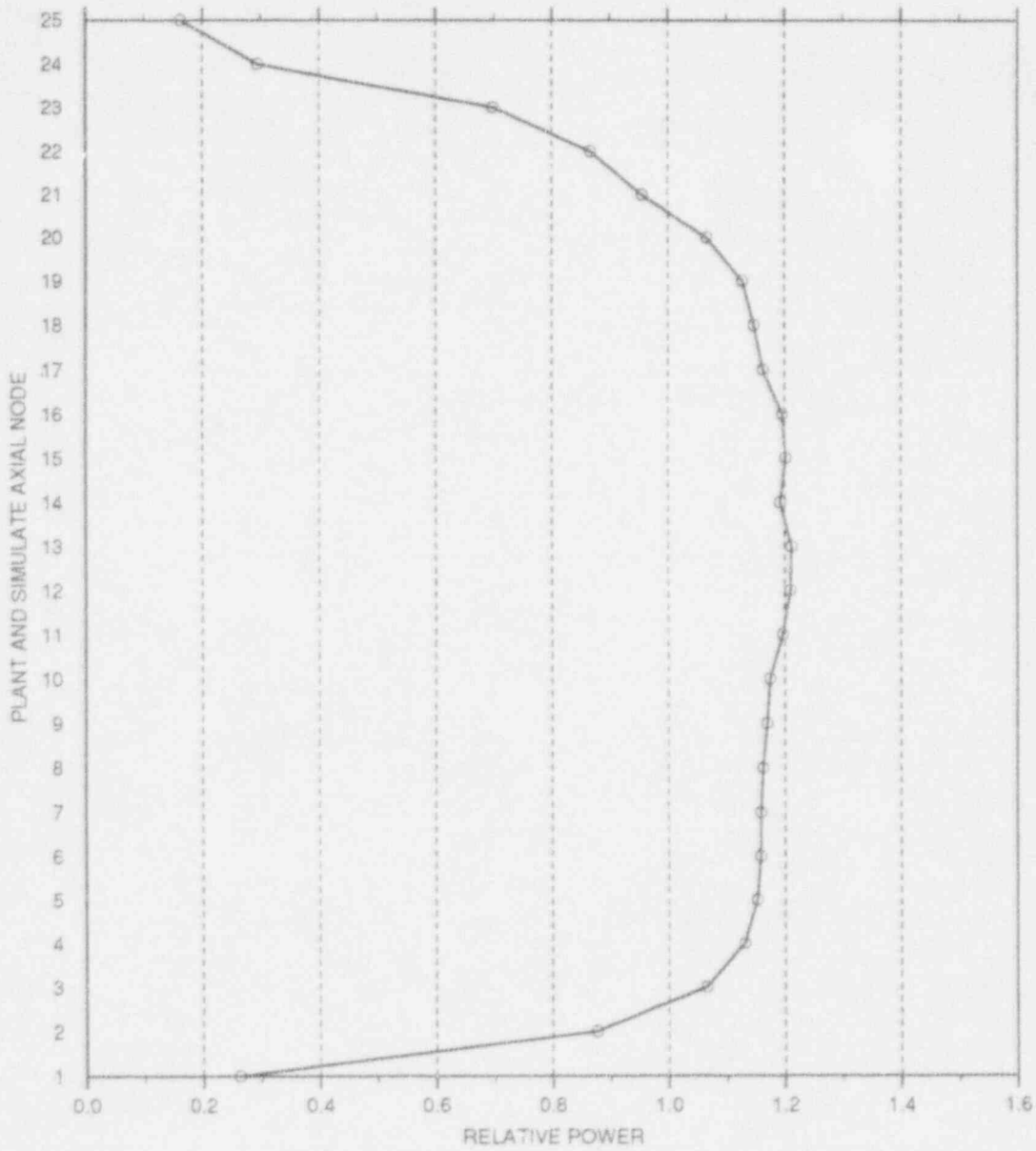

FIGURE 5.1.2

VY CYCLE 17 HALING DEPLETION, EOFPL CORE AVERAGE AXIAL POWER DISTRIBUTION

FIGURE 5.1.3

VY CYCLE 17 RODDED DEPLETION - 7[illegible]0 AT EOFPL, BUNDLE AVERAGE RELATIVE POWERS

FIGURE 5.1.4

VY CYCLE 17 RODDED DEPLETION - ARO AT EOFPL,
CORE AVERAGE AXIAL POWER DISTRIBUTION

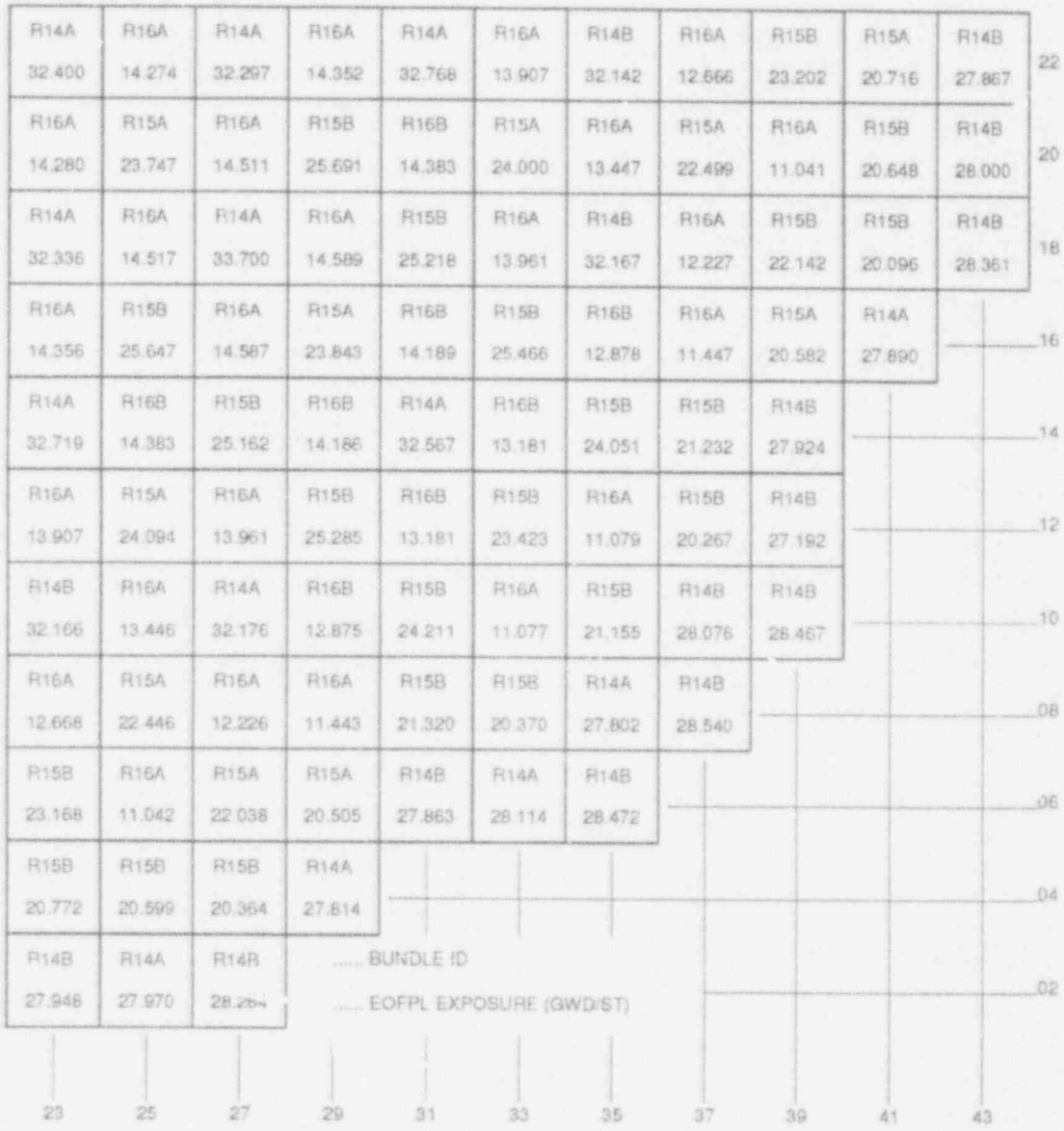

FIGURE 5.2.1

VY CYCLE 17 HALING DEPLETION, EOFPL BUNDLE AVERAGE EXPOSURES

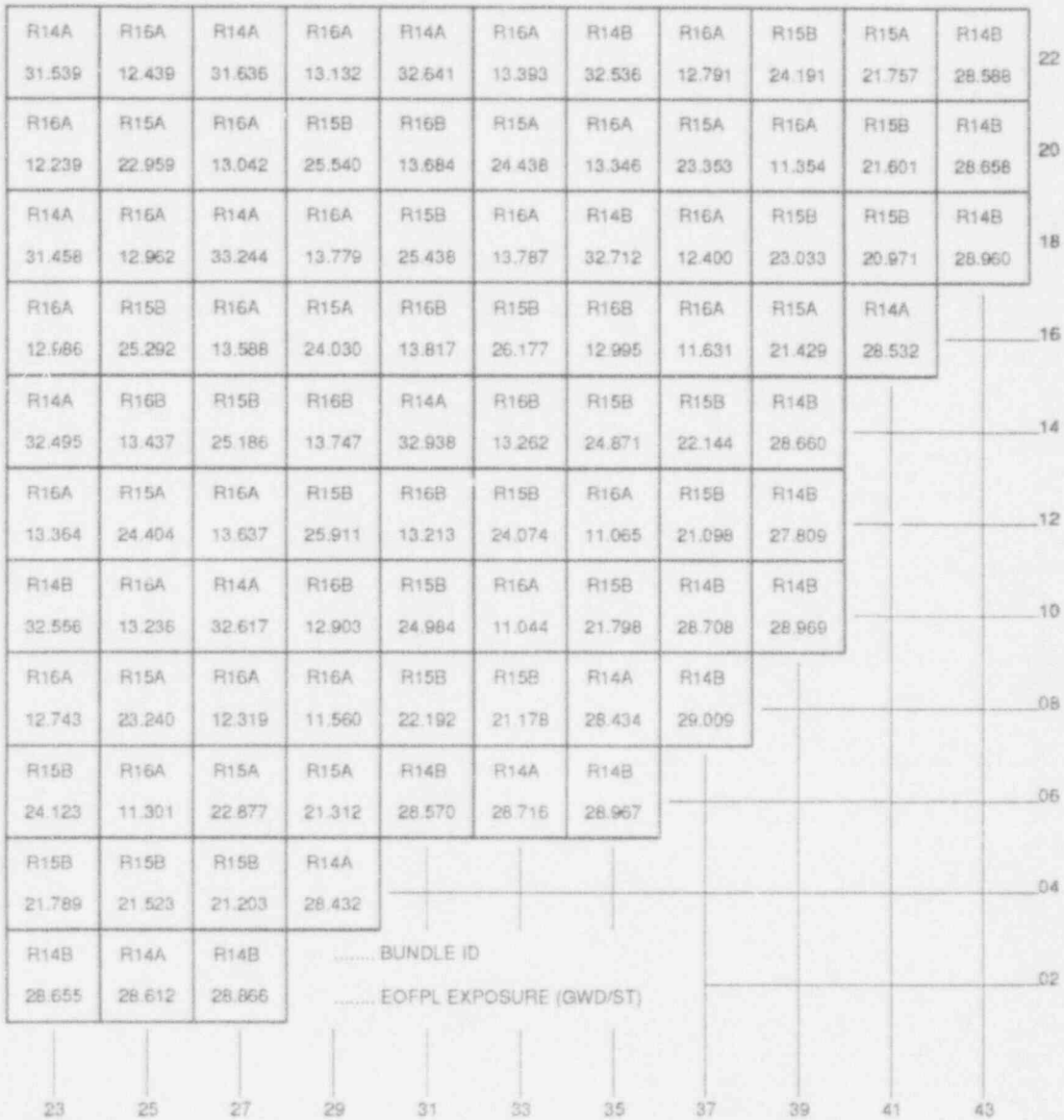

FIGURE 5.2.2

VY CYCLE 17 RODDED DEPLETION, EOFPL BUNDLE AVERAGE EXPOSURES

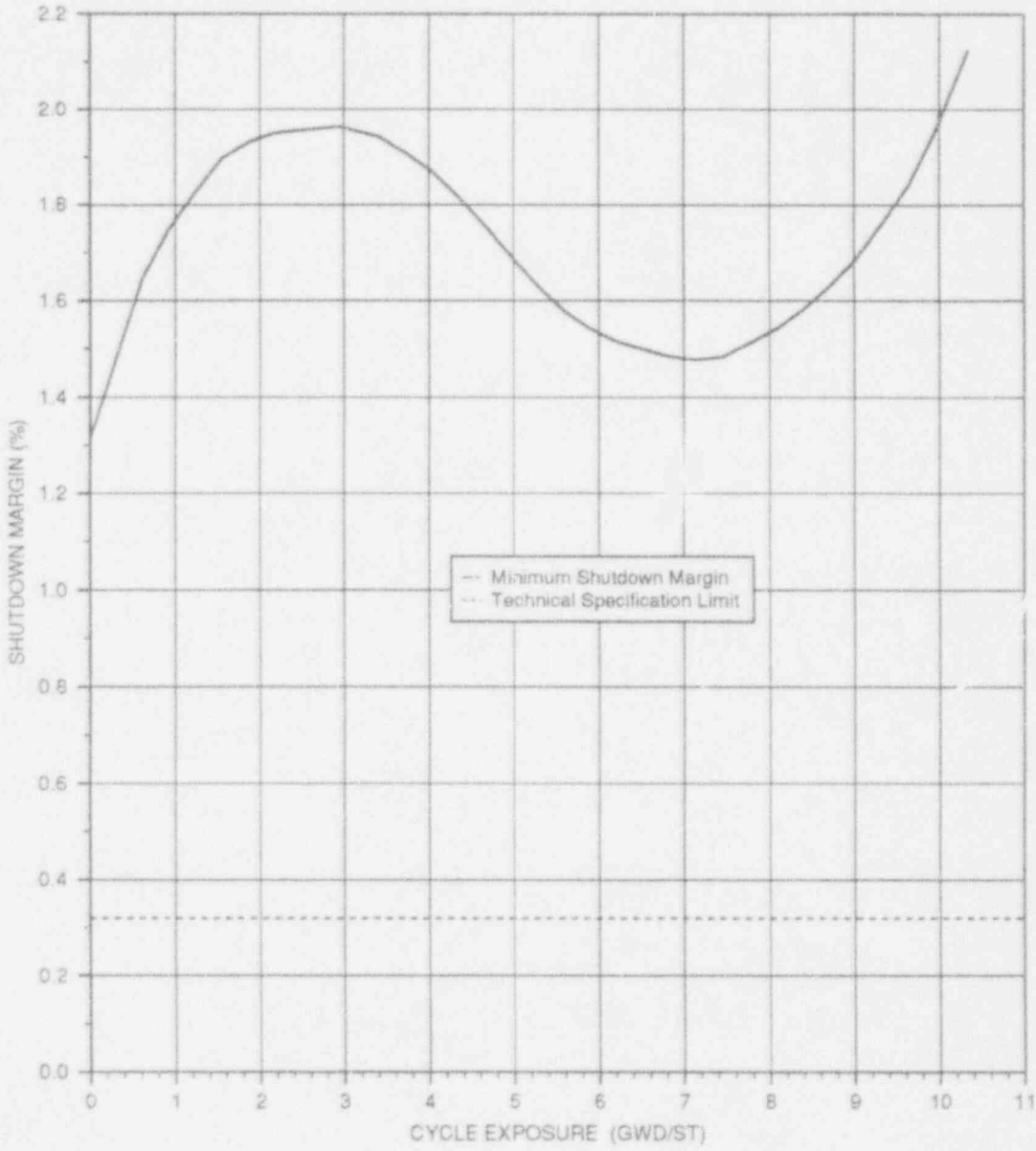

FIGURE 5.3.1

VY CYCLE 17 COLD SHUTDOWN MARGIN, IN %ΔK, VERSUS CYCLE EXPOSURE

6.0 THERMAL-HYDRAULIC DESIGN

6.1 Steady-State Thermal Hydraulics

Core steady-state thermal-hydraulic analyses for the Reload Cycle were performed using the FIBWR[16],[17],[18] computer code. The FIBWR code incorporates a detailed geometrical representation of the complex flow paths in a BWR core, and explicitly models the leakage flow to the bypass region and water rod flow. The FIBWR geometric models for each GE bundle type were benchmarked against vendor-supplied and plant thermal-hydraulic information.

Using the fuel bundle geometric models, a power distribution calculated by SIMULATE-3 and core inlet enthalpy, the FIBWR code calculates the core pressure drop and total bypass flow for several power and flow combinations. The core pressure drop and total bypass flow predicted by the FIBWR code were then used in setting the initial conditions for the system transient analysis model.

6.2 Reactor Limits Determination

Vermont Yankee Technical Specifications [12] has Limiting Conditions for Operation associated with the fuel rods. These limits are Minimum Critical Power Ratio (MCPR), Maximum Linear Heat Generation Rate (MLHGR) and Maximum Average Linear Heat Generation Rate (MAPLHGR).

The objective for normal operation and anticipated transient events is to maintain nucleate boiling. Avoiding a transition to film boiling protects the fuel cladding integrity. The Fuel Cladding Integrity Safety Limit (FCISL) for Vermont Yankee is a Critical Power Ratio (CPR) of 1.07 [2]. CPR is defined as the ratio of the critical power (bundle power at which some point within the assembly experiences onset of boiling transition) to the operating bundle power. Thermal margin is stated in terms of the minimum value of the MCPR which corresponds to the most limiting fuel assembly in the core. Both the transient (safety) and normal MCPR operating thermal limits

are derived with the GEXL-Plus correlation[19], with appropriate coefficients representative of the Reload Cycle's hot assembly fuel type. The MCPR limits for the Reload Cycle are found in Appendix A.

The MLHGR limit for the Reload Cycle is 14.4 kW/ft for all bundle types. The basis for the MLHGR limit can be found in the fuel mechanical analysis in Reference 2.

The MAPLHGR limits for the Reload Cycle are shown in Appendix A. They are the most limiting of the fuel mechanical analysis MAPLHGRs[20] and the LOCA analysis MAPLHGRs (Section 8.2). The fuel mechanical design analysis, using the methods in Reference 2, demonstrate that all fuel rods in a lattice, operating at the bounding power history, meet the fuel design limits specified in Reference 2. The transients, described in Section 7.0, were analyzed to verify that the thermal and mechanical overpower design criteria[21] in the mechanical design analysis methods are not exceeded. The LOCA analysis is described in Section 8.0.

7.0 ABNORMAL OPERATIONAL TRANSIENT ANALYSIS

7.1 Transients Analyzed

Transient simulations are performed to assess the impact of certain transients on the heat transfer characteristics of the fuel. The purpose of this analysis is: 1) to determine the MCPR operating limit so that the FCISL is not violated for the transients considered, 2) to assure that the fuel mechanical design criteria are not exceeded during the transient, and 3) to demonstrate compliance with the ASME vessel code limits.

Past licensing analysis has shown that the transients which result in the maximum MCPR are:

1. Pressurization transients, including the generator load rejection with complete failure of the turbine bypass system and the turbine trip with complete failure of the turbine bypass system;

2. Loss of feedwater heating;

3. Local rod withdrawal error; and

4. Misloaded bundle error, including the rotated bundle error and the mislocated bundle error.

The "feedwater controller failure" (maximum demand) transient is not a limiting transient for Vermont Yankee, because of the plant's 110% steam flow bypass capacity. Past analyses have shown this transient to be considerably less limiting than any of the above for all exposure points. The events reported herein are limiting; no other transients would produce more restrictive MCPR operating limits for the Reload Cycle.

To demonstrate the fuel mechanical design criteria is met the maximum powers resulting from the pressurization, loss of feedwater

heating and rod withdrawal error transients were compared to the criteria. To demonstrate compliance with ASME vessel code limits the main steam isolation valves (MSIV) closing with failure of the MSIV position switch is also analyzed. Brief descriptions and the results of the transients analyzed are provided in the following sections.

7.2 Pressurization Transients Analysis

7.2.1 Methodology

The analysis involves two types of simulations. A system level simulation is performed to determine the overall plant response. Transient core inlet and exit conditions and normalized power from the system level calculation are then used to perform detailed thermal-hydraulic simulations of the fuel, referred to as "hot channel calculations." The hot channel simulations provide the bundle transient ΔCPR (the initial bundle CPR minus the MCPR experienced during the transient).

The system level simulations are performed with the one dimensional (1-D) kinetics RETRAN model[22],[23],[24]. The hot channel calculations are performed with the RETRAN[25],[26] and TCPYA01[27],[18],[23] computer codes. The GEXL-Plus correlation [19], contained in TCPYA01, evaluates the transient critical power ratio.

The hot channel transient ΔCPR calculations employ a two-part process, as illustrated by the flow chart in Figure 7.2.1. The first part involves a series of steady-state analyses performed with the FIBWR, RETRAN, and TCPYA01 computer codes. The FIBWR analyses utilize a one-channel model for each fuel type being analyzed, with bypass and water rod flow also modeled. The steady-state FIBWR analyses were performed at several power levels with other conditions (i.e., core pressure drop, system pressure, and core inlet enthalpy) held constant. The FIBWR code results provide a steady-state CPR, active channel flow (AF) and bypass flow (BPF) for each active channel power (AP).

The FIBWR conditions for channel power, channel flow, and bypass flow were then used as input to steady-state RETRAN/TCPYA01 hot channel calculations. Other assumptions are consistent with those in the FIBWR analysis. The Initial Critical Power Ratio (ICPR) is the result of the steady-state RETRAN/TCPYA01 analysis. These results allow for the development of functional relationships, describing AP as a function of ICPR, and AF and BPF as functions of AP for each fuel type. These relationships are used in the iterative process for determining the transient CPR, as shown in Figure 7.2.1.

The second part of the hot channel calculations determines the transient CPR performance. Because the ΔCPR for a given transient varies with Initial Critical Power Ratio (ICPR), the hot channel analysis is an iterative process. The objective of the hot channel iteration for each transient is to determine the hot channel initial conditions which result in reaching the FCISL. Each iteration requires a RETRAN hot channel run to calculate the transient enthalpies, flows, pressure and saturation properties at each time step. These are required for input to the TCPYA01 code. TCPYA01 is then used to calculate a CPR at each time step during the transient, from which a transient ΔCPR is derived.

The NRC Safety Evaluation for FROSSTEY-2 [11] required that the analysis assume the worst axial power shape prior to the transient for core wide and hot channel analyses. In addition, the hot channel methodology has considered the assumption of both fixed and time-varying power shapes. The fixed power shape assumes a 1.4 chopped cosine axial distribution which remains constant throughout the transient. The initial power shape assumed in the time-varying power shape analysis is the Haling axial distribution used in the core wide analysis. The time-varying hot channel power distribution is assumed to be the same as that in the core wide analysis calculated from the 1-D kinetics representation. The transient MCPR limits are defined as the more conservative results from the fixed and varying shape analyses.

7.2.2 Initial Conditions and Assumptions

The initial conditions for the Reload Cycle are based on a reactor power level of 1664 MW_{th} which includes a 4.5% margin on the current licensed reactor power level of 1593 MW_{th}. This margin conservatively bounds the expected 2% calorimetric uncertainty. The reactor core flow is assumed to be 100% of rated. The core axial power distribution for each of the exposure points is based on the 3-dimensional SIMULATE-3 predictions associated with the generation of the reactivity data (Section 7.2.3). The core inlet enthalpy is set so that the amount of carryunder from the steam separators and the quality in the liquid region outside the separators is as close to zero as possible. For fast pressurization transients, this maximizes the initial pressurization rate and results in a more severe neutron power spike. A summary of the initial operating state used for the system simulations is provided in Table 7.2.1.

During the cycle, Vermont Yankee can adjust the core flow to account for reactivity changes rather than using the control rods. During this type of operation, core flow may be as low as 87% while at 100% power. To ensure the safety analysis bounds these conditions, transients are also analyzed at the limiting exposure statepoint at 1664 MW_{th} power and 87% flow. Limiting exposure is defined as the exposure which had the highest increase in ΔCPR.

Assumptions specific to a particular transient are discussed in the section describing the transient. In general, the following assumptions are made for all transients:

1. Scram setpoints are at Technical Specification [12] limits.

2. Protective system logic delays are at equipment specification limits.

3. Safety/relief valve and safety valve capacities are based on Technical Specification rated values.

4. Safety/relief valve and safety valve setpoints are modeled as being at the Technical Specification upper limit. Valve responses are based on slowest specified response values.

5. Control rod drive scram speed is based on the Technical Specification limits. The analysis addresses a dual set of scram speeds, referred to as the "Measured" and the "67B" scram times. "Measured" refers to the faster scram times given in Section 3.3.C.1.1 of the Technical Specifications. "67B" refers to the slower scram times given in Section 3.3.C.1.2 of the Technical Specifications.

7.2.3 One-Dimensional Cross Sections and Kinetics Parameters

The one-dimensional (1-D) cross sections and kinetics parameters are generated as functions of fuel temperature, moderator density, and scram. The method[28] is outlined below.

A complete set of 1-D cross sections, kinetics parameters, and axial power distributions are generated from base states using the Haling depletion established for EOFPL, EOFPL-1000 MWd/St, EOFPL-2000 MWd/St, and BOC exposure statepoints. These statepoints are characterized by exposure and void history distributions, control rod patterns, and core thermal-hydraulic conditions. The latter are consistent with the assumed system transient conditions provided in Table 7.2.1.

The BOC base state is established by shuffling from the previously defined Current Cycle endpoint into the Reload Cycle loading pattern. A criticality search provides an estimate of the BOC critical rod pattern. The EOFPL and intermediate core exposure and void history distributions are calculated with a Haling depletion as described in Section 5.2. The EOFPL state is unrodded. The EOFPL-1000 MWd/St and EOFPL-2000 MWd/St exposure statepoints require base control rod patterns. These are developed to be as "black and white" as possible to minimize the scram reactivity, maximize the core average moderator density reactivity coefficient and, therefore,

maximize the transient power response. Beginning with the rodded depletion configuration, all control rods which are more than half inserted are fully inserted, and all control rods which are less than half inserted are fully withdrawn. If the SIMULATE-3 calculated parameters are within operating limits, then this configuration becomes the base case. If the limits are exceeded, a minimum number of control rods are adjusted a minimum number of notches until the parameters fall within limits.

At each exposure statepoint, a SIMULATE-3 initial control state reference case is run. A series of perturbation cases are run with SIMULATE-3 to independently vary the fuel temperature, moderator temperature, and core pressure. All other variables normally associated with the SIMULATE-3 cross sections are held constant at the reference state. To obtain the effect of the control rod scram, another SIMULATE-3 reference case is run with all-rods-in. The perturbation cases described above are run again from this reference case. For each control state, a data set of kinetics parameters and cross sections is generated as a function of the perturbed variable. There is a table set for each of the 27 neutronic regions, 25 regions to represent the active core and one region each for the bottom and top reflectors.

7.2.4 Turbine Trip Without Bypass Transient (TTWOBP)

The transient is initiated by a rapid closure (0.1 second closing time) of the turbine stop valves. It is assumed that the steam bypass valves, which normally open to relieve pressure, remain closed. A reactor protection system signal is generated by the turbine stop valve closure switches. Control rod drive motion is conservatively assumed to occur 0.27 seconds after the start of turbine stop valve motion. The ATWS recirculation pump trip is assumed to occur at a setpoint of 1150 psig dome pressure. A pump trip time delay of 1.0 second is assumed to account for logic delay and M-G set generator field collapse. In simulating the transient, the bypass piping volume up to the valve chest is lumped into the control volume upstream of the turbine stop valves. Predictions of the salient system parameters

at the three exposure points are shown in Figures 7.2.2 through 7.2.4 for the "Measured" scram time analysis.

7.2.5 Generator Load Rejection Without Bypass Transient (GLRWOBP)

The transient is initiated by a rapid closure (0.3 seconds closing time) of the turbine control valves. As in the case of the turbine trip transient, the bypass valves are assumed to fail. A reactor protection system signal is generated by the hydraulic fluid pressure switches in the acceleration relay of the turbine control system. Control rod drive motion is conservatively assumed to occur 0.28 seconds after the start of turbine control valve motion. The same modeling regarding the ATWS pump trip and bypass piping is used as in the turbine trip simulation. The influence of the accelerating main turbine generator on the recirculation system is simulated by specifying the main turbine generator electrical frequency as a function of time for the M-G set drive motors. The main turbine generator frequency curve is based on a 100% power plant startup test and is considered representative for the simulation. The system model predictions for the three exposure points are shown in Figures 7.2.5 through 7.2.7 for the "Measured" scram time analysis.

7.2.6 Pressurization Transient Analysis Results

The transients selected for consideration were analyzed at exposure points of EOFPL, EOFPL-1000 MWd/St, and EOFPL-2000 MWd/St. The transient results, reported in Table 7.2.2, correspond to the limiting bundle type in the core. The MCPR limits, in Table 7.2.2, are calculated by adding the calculated ΔCPR to the FCISL. The worst ΔCPR for the pressurization transients include an adjustment to allow for the exposure window of ±600 MWd/St on Current Cycle and the exposure uncertainty on the Reload Cycle[7].

7.3 Loss of Feedwater Heating Transient (LOFWH) Results

A feedwater heater can be lost in such a way that the steam extraction line to the heater is shut off or the feedwater flow

bypasses one of the heaters. In either case, the reactor will receive cooler feedwater, which will produce an increase in the core inlet subcooling, resulting in a reactor power increase.

The response of the system due to the loss of 100°F of the feedwater heating capability was analyzed. This represents the maximum expected feedwater temperature reduction for a single heater or group of heaters that can be tripped or bypassed by a single event. The system model used is the same as that used for the pressurization transient analysis (Section 7.2.1). The initial conditions and modeling assumptions discussed in Section 7.2.2 are applicable to this simulation.

Vermont Yankee has a scram setpoint of 120% of rated power as part of the Reactor Protection System (RPS) on high neutron flux. In this analysis, no credit was taken for scram on high neutron flux, thereby allowing the reactor power to reach its peak without scram. This approach was selected to provide a bounding and conservative analysis for events initiated from any power level.

The transient response of the system was evaluated at several exposures during the cycle: EOFPL, EOFPL-1000 MWd/St, EOFPL-2000 MWd/St, and BOC. The transient results, corresponding to the limiting bundle type in the core, are listed in Table 7.3.1. The MCPR limits in Table 7.3.1 are calculated by adding the calculated ΔCPR to the FCISL. The transient evaluation at BOC was found to be the limiting case between BOC to EOFPL. The results of the system response to a loss of 100°F feedwater heating capability evaluated at BOC as predicted by the RETRAN code are presented in Figure 7.3.1.

7.4 Overpressurization Analysis Results

Compliance with ASME vessel code limits is demonstrated by an analysis of the Main Steam Isolation Valves (MSIV) closing with failure of the MSIV position switch scram. EOFPL conditions were analyzed. The system model used is the same as that used for the transient analysis (Section 7.2.1). The initial conditions and

modeling assumptions discussed in Section 7.2.2 are applicable to this simulation.

The transient is initiated by a simultaneous closure of all MSIVs. A 3.0 second closing time, which is the minimum time in Technical Specification Table 4.7.2, is assumed. A reactor scram signal is generated on APRM high flux. Control rod drive motion is conservatively assumed to initiate 0.28 seconds after reaching the high flux setpoint. The system response is shown in Figure 7.4.1 for the "Measured" scram time analysis.

The maximum pressures at the bottom of the reactor vessel calculated for the "Measured" scram time analysis and for the "67B" scram time analysis are given in Table 7.4.1. These results are within the ASME code overpressure design limit which is 110% of the vessel design pressure. Vermont Yankee's design pressure is 1250 psig so the maximum pressure limit is 1375 psig.

7.5 Local Rod Withdrawal Error Transient Results

The rod withdrawal error (RWE) is a local core transient caused by an operator erroneously withdrawing a control rod in the continuous withdrawal mode. If the core is operating at its operating limits for MCPR at the time of the error, then withdrawal of a control rod could increase both local and core power levels with the potential for overheating the fuel.

There is a broad spectrum of core conditions and control rod patterns which could be present at the time of such an error. For most normal situations it would be possible to fully withdraw a control rod without violating the FCISL.

The MCPR operating limit for the RWE is defined at each Rod Block Monitor (RBM) System setpoint so that the FCISL is not violated. The consequences of the error depend on the local power increase, the initial MCPR of the neighboring locations and the ability of the RBM to stop the withdrawing rod before MCPR reaches the FCISL.

The most severe transient postulated begins with the core operating according to normal procedures and within normal operating limits. The operator makes a procedural error and attempts to fully withdraw the maximum worth control rod at maximum withdrawal speed. The core limiting locations are close to the error rod. They experience the spatial power shape transient as well as the overall core power increase.

The core conditions and control rod pattern are conservatively modeled for the licensing bounding case by specifying the following set of concurrent worst case assumptions:

1. The rod should have high reactivity worth. The worst rod is identified by running the full RWE analysis for the control rods as found in the normal control rod patterns of the rodded depletion. Every control rod sequence is checked. From this examination, the control rods that result in the highest worth and highest ΔCPR are identified. Licensing test case rod patterns are then developed to further exaggerate the worth and ΔCPR impact of the rod to be withdrawn.

   The test patterns are developed with xenon-free conditions. The xenon-free condition and the additional control rod inventory needed to maintain criticality exaggerates the worth of the withdrawn control rod when compared to normal operation with normal xenon levels.

2. The core is modeled at 104.5% power and 100% flow.

3. The core power distribution is adjusted with the available control rods to place the locations within the four by four array of bundles around the error rod as close to the operating limits as possible.

4. Of the many patterns tested, the pattern with the most limiting ΔCPR results is selected as the bounding case.

The RBM System's ability to terminate the bounding case is evaluated on the following bases:

1. Technical Specifications allow each of the separate RBM channels to remain operable if at least half of the Local Power Range Monitor (LPRM) inputs on each level are operable. For the interior locations tested in this analysis, there are a maximum of four LPRM inputs per level. One RBM channel averages the inputs from the A and C levels; the other channel averages the inputs from the B and D levels. Considering the inputs for a single channel, there are eleven failure combinations of none, one and two failed LPRM strings. The RBM channel responses are evaluated separately at these eleven input failure conditions. Then, for each channel taken separately, the lowest response as a function of error rod position is chosen for comparison to the RBM setpoint.

2. The event is analyzed separately in each of the four quadrants of the core due to the differing LPRM string physical locations relative to the error rod.

Technical Specifications require that both RBM channels be operable during normal operation. Thus, the first channel calculated to intercept the RBM setpoint is assumed to stop the rod. To allow for control system delay times, the rod is assumed to move two inches after the intercept and stop at the following notch.

The analysis is performed using SIMULATE-3. The two separate cases presented here are selected from numerous explicit SIMULATE-3 analyses. The reactor conditions and case descriptions are shown in Figures 7.5.1 and 7.5.2. Case 1 analyzes the bounding event with zero xenon, initiated from 104.5% power, for the worst case abnormal rod pattern configuration. Case 2 is the worst of the normal control rod patterns found in the rodded depletion, initiated from 100% power conditions and equilibrium xenon. The transient ΔCPR results are also shown in Figures 7.5.1 and 7.5.2. The ΔCPR values are evaluated such

that the implied MCPR operating limit equals FCISL + ΔCPR. This is done by conserving the figure of merit (ΔCPR/ICPR) shown by the SIMULATE-3 calculations. The use of this method provides valid ΔCPR values in the analysis of normal operating states where locations near the assumed error rod are not initially near the MCPR operating limit.

Case 2 is the worst of all the rod withdrawal transients analyzed from 100% power, full flow and normal rod pattern conditions. Case 2 is bounded by Case 1 by at least 0.02 ΔCPR margin to assure that the exposure uncertainties on the Current Cycle and the Reload Cycle are accounted for.

The Case 1 (bounding event) RBM channel responses are shown in Figures 7.5.3 and 7.5.4. They also show the control rod position at the point where the weakest RBM channel response first intercepts the RBM setpoint. For this same bounding case, the operating limit ΔCPR envelope component versus RBM setpoint is taken from Figure 7.5.1.

7.6 Misloaded Bundle Error Analysis Results

7.6.1 Rotated Bundle Error

The primary result of a bundle rotation is a large increase in local pin peaking and the associated R-factor as higher enrichment pins are placed adjacent to the surrounding wide water gaps. In addition, there may be a small increase in reactivity, depending on the exposure and void fraction states. The R-factor increase results in a CPR reduction. The objective of the analysis is to ensure that, in the worst possible rotation, the FCISL is not violated with the most limiting bundles on their operating limits.

To analyze the CPR response, rotated bundle R-factors as a function of exposure are developed by adding the largest possible ΔR-factor resulting from a rotation to the exposure dependent R-factors of the properly oriented bundles. Using these rotated bundle R-factors, the MCPR values resulting from a bundle rotation are determined using SIMULATE-3. This is done for each control rod

sequence throughout the cycle. The process is repeated with the K-infinity of the limiting bundle modified slightly to account for the increase in reactivity resulting from the rotation. For each sequence, the MCPR for the properly oriented bundles is adjusted by a ratio necessary to place the corresponding rotated bundle's CPR on its FCISL. The adjusted MCPRs at each exposure is the rotated bundle operating limit for the rotated bundle error.

Because the BP8DWB335 fuel designs exhibit a significant increase in R-factor with rotation early in exposure, the impact upon the rotated bundle ΔCPR is high at BOC. This effect soon drops off with exposure. Therefore, the operating MCPR limit resulting from a rotation is presented in Table 7.6.1 versus cycle exposure.

7.6.2 Mislocated Bundle Error

Misloading a high reactivity assembly into a region of high neutron importance results in a location of high relative assembly average power. Since the assembly is assumed to be properly oriented (not rotated), R-factors used for the misloaded bundle are the standard values for the given fuel type.

The analysis uses multiple SIMULATE-3 cases to examine the effects of explicitly mislocating every older interior assembly in a quarter core with a fresh or once-burned assembly. Because of symmetry, the results apply to the whole core. Edge bundles are not examined because they are never limiting, due to neutron leakage.

The effect of the successive mislocations is examined for every control rod sequence throughout the cycle. For each sequence, the MCPR for the properly loaded core is compared to the MCPR of the misloaded core at the misloaded location. The MCPR for the properly loaded core is adjusted by a ratio necessary to place the mislocated assembly on the FCISL. The maximum of these adjusted MCPRs is the mislocated bundle operating limit. The results of the mislocated bundle analysis are given in Table 7.6.2.

TABLE 7.2.1

VY CYCLE 17 SUMMARY OF SYSTEM TRANSIENT MODEL
INITIAL CONDITIONS FOR TRANSIENT ANALYSES

Core Thermal Power (MW_{th})	1664.0
Turbine Steam Flow ($10^6 lb_m/hr$)	6.75
Total Core Flow ($10^6 lb_m/hr$)	48.0
Core Bypass Flow ($10^6 lb_m/hr$)*	6.29
Core Inlet Enthalpy (BTU/lb_m)	523.2
Steam Dome Pressure (psia)	1034.7
Turbine Inlet Pressure (psia)	985.7
Total Recirculation Drive Flow ($10^6 lb_m/hr$)	23.8
Core Plate Differential Pressure (psi)	20.49
Narrow Range Water Level (in.)	162.0
Average Fuel Gap Conductance	(See Section 4.2)

* Includes water rod flow.

TABLE 7.2.2

VY CYCLE 17 PRESSURIZATION TRANSIENT ANALYSIS RESULTS

Transient	Exposure Statepoint	Peak Prompt Power (Fraction of Initial Value)	Peak Average Heat Flux (Fraction of Initial Value)	ΔCPR*	Transient MCPR Limits
Turbine Trip Without Bypass, "Measured" Scram Time	EOFPL	2.724	1.194	0.24	1.31
	EOFPL-1000	2.179	1.139	0.20	1.27
	EOFPL-2000	1.223	1.000	0.05	1.12
Turbine Trip Without Bypass, "67B" Scram Time	EOFPL	3.116	1.229	0.26	1.33
	EOFPL-1000	2.620	1.183	0.22	1.29
	EOFPL-2000	1.526	1.040	0.07	1.14
Generator Load Rejection Without Bypass, "Measured" Scram Time	EOFPL	2.632	1.181	0.25	1.32
	EOFPL-1000	2.254	1.129	0.19	1.26
	EOFPL-2000	1.197	1.000	0.03	1.10
Generator Load Rejection Without Bypass, "67B" Scram Time	EOFPL	3.088	1.232	0.27	1.34
	EOFPL-1000	2.679	1.187	0.23	1.30
	EOFPL-2000	1.548	1.029	0.06	1.13

* The worst ΔCPR for TTWOBP and GLRWOBP includes a 0.01 ΔCPR adjustment to allow for the exposure window of ±600 MWd/St on Current Cycle and the exposure uncertainty on the Reload Cycle.

TABLE 7.3.1

VY CYCLE 17 LOSS OF FEEDWATER HEATING TRANSIENT ANALYSIS RESULTS

Transient	Exposure Statepoint	Peak Prompt Power (Fraction of Initial Value)	Peak Average Heat Flux (Fraction of Initial Value)	ΔCPR	Transient MCPR Limits
Loss of 100°F Feedwater Heating	EOFPL	1.180	1.182	0.16	1.23
	EOFPL-1000	1.256	1.183	0.16	1.23
	EOFPL-2000	1.254	1.182	0.14	1.21
	BOC	1.182	1.183	0.16	1.23

TABLE 7.4.1

VY CYCLE 17 OVERPRESSURIZATION ANALYSIS RESULTS

Conditions	Maximum Pressure at Reactor Vessel Bottom (psig)
"Measured" Scram Time	1235.2
"67B" Scram Time	1260.7

TABLE 7.6.1

VY CYCLE 17 ROTATED BUNDLE ANALYSIS RESULTS

Exposure (GWd/St)	Transient MCPR Limit
0 - 4.0	1.42
4.0 - 5.5	1.34
5.5 - 6.5	1.28
6.5 - EOFPL	1.21

TABLE 7.6.2

VY CYCLE 17 MISLOCATED BUNDLE ANALYSIS RESULTS

Transient MCPR Limit
1.19

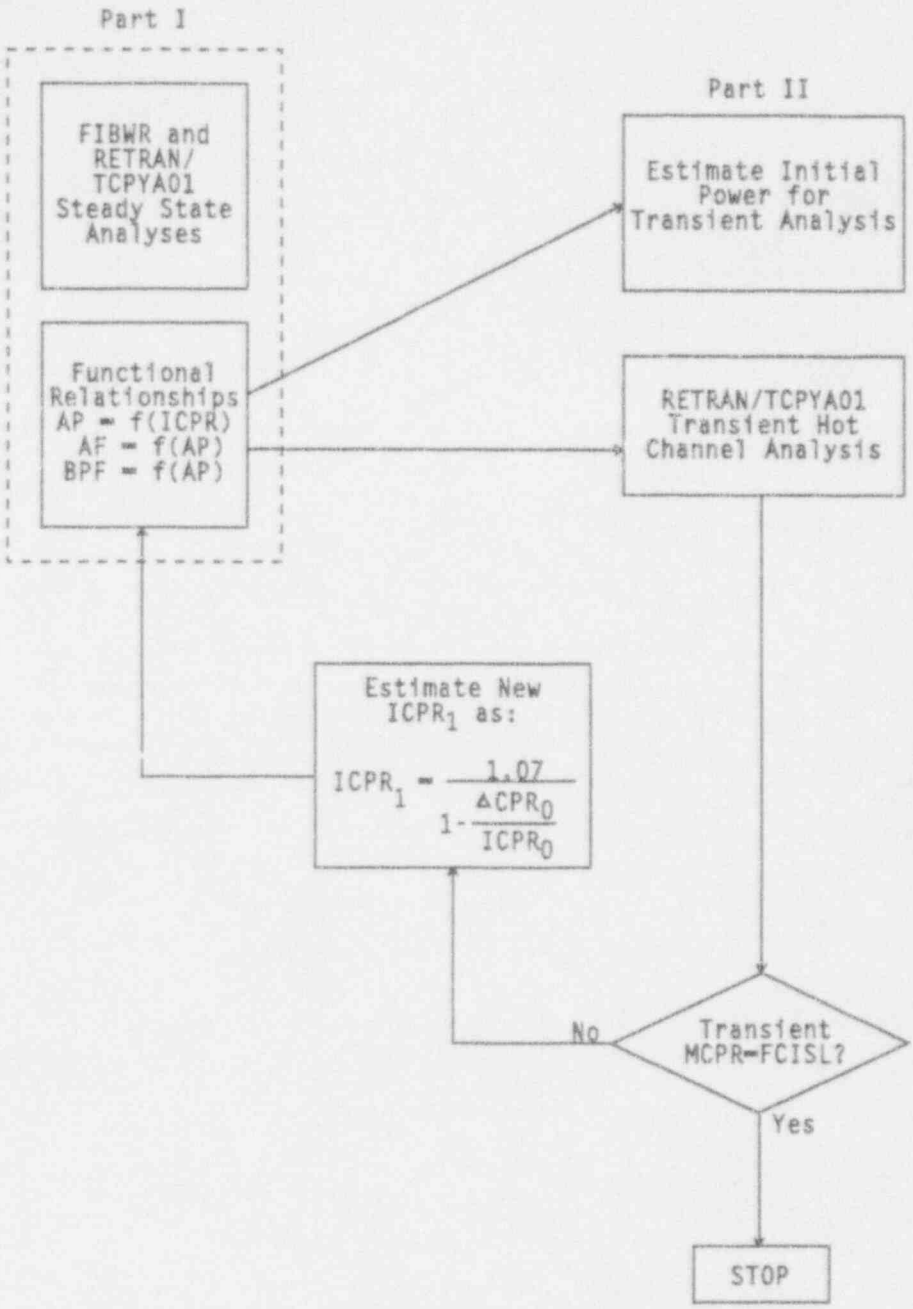

FIGURE 7.2.1

FLOW CHART FOR THE CALCULATION OF ΔCPR USING THE RETRAN/TCPYA01 CODES

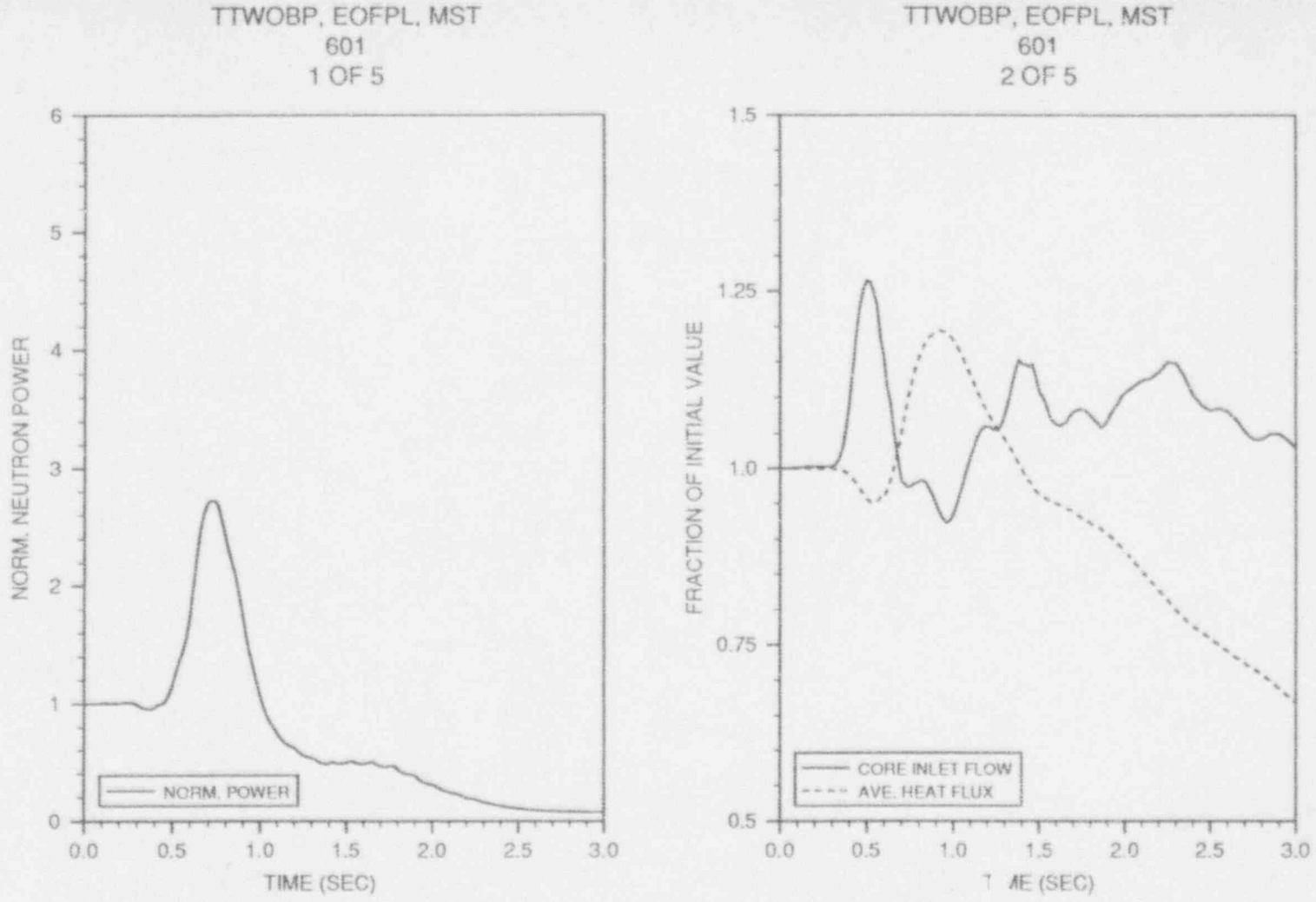

FIGURE 7.2.2

TURBINE TRIP WITHOUT BYPASS, EOFPL17
TRANSIENT RESPONSE VERSUS TIME, "MEASURED" SCRAM TIME

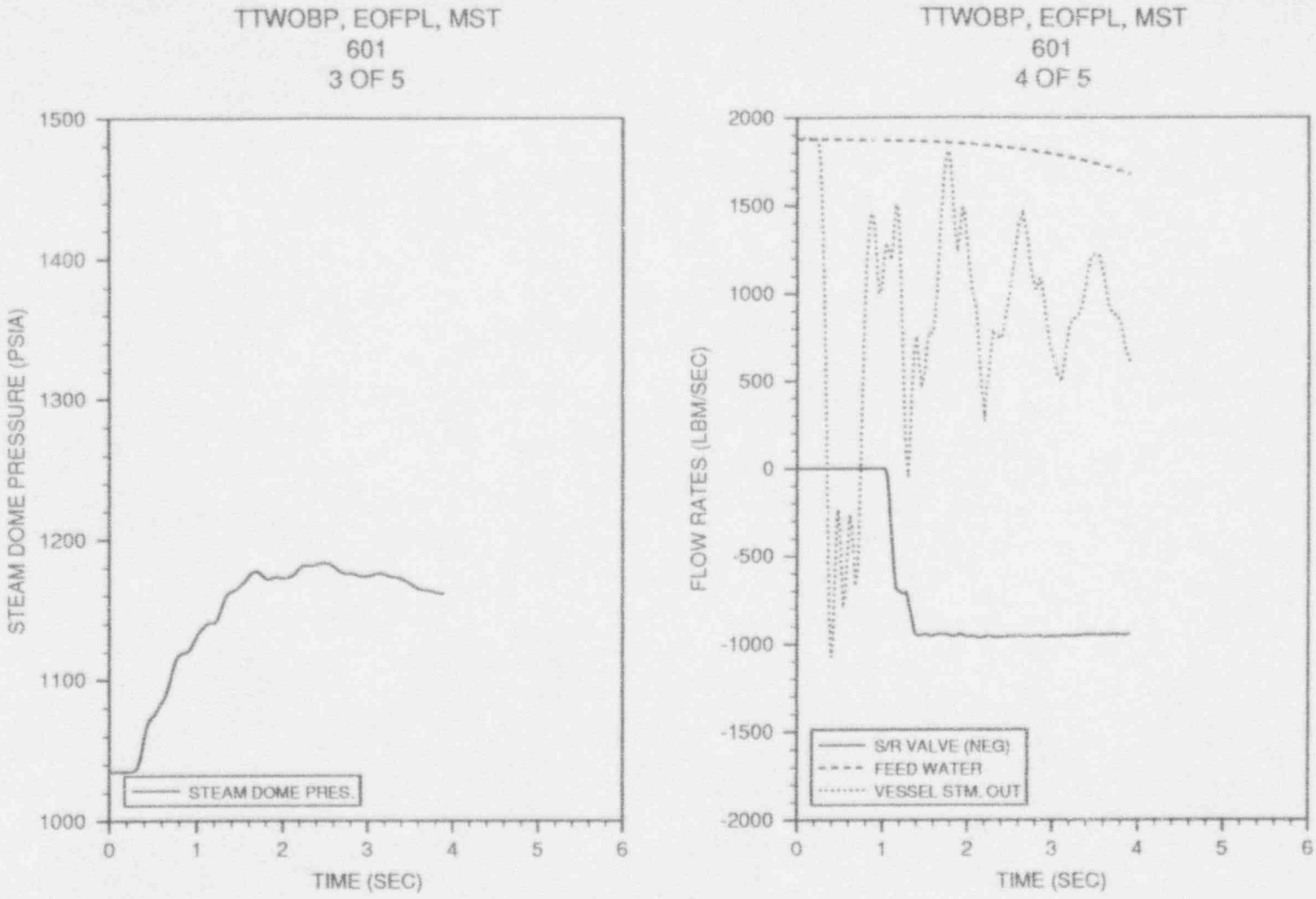

FIGURE 7.2.2
(Continued)

TURBINE TRIP WITHOUT BYPASS, EOFPL17
TRANSIENT RESPONSE VERSUS TIME, "MEASURED" SCRAM TIME

TTWOBP, EOFPL, MST
601
5 OF 5

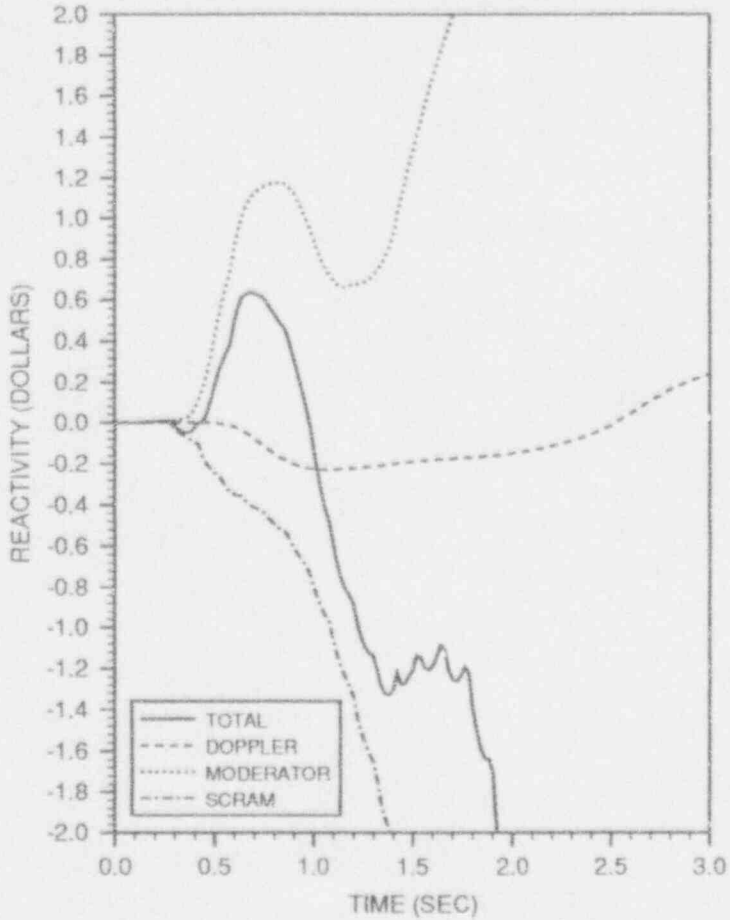

FIGURE 7.2.2
(Continued)

TURBINE TRIP WITHOUT BYPASS, EOFPL17
TRANSIENT RESPONSE VERSUS TIME, "MEASURED" SCRAM TIME

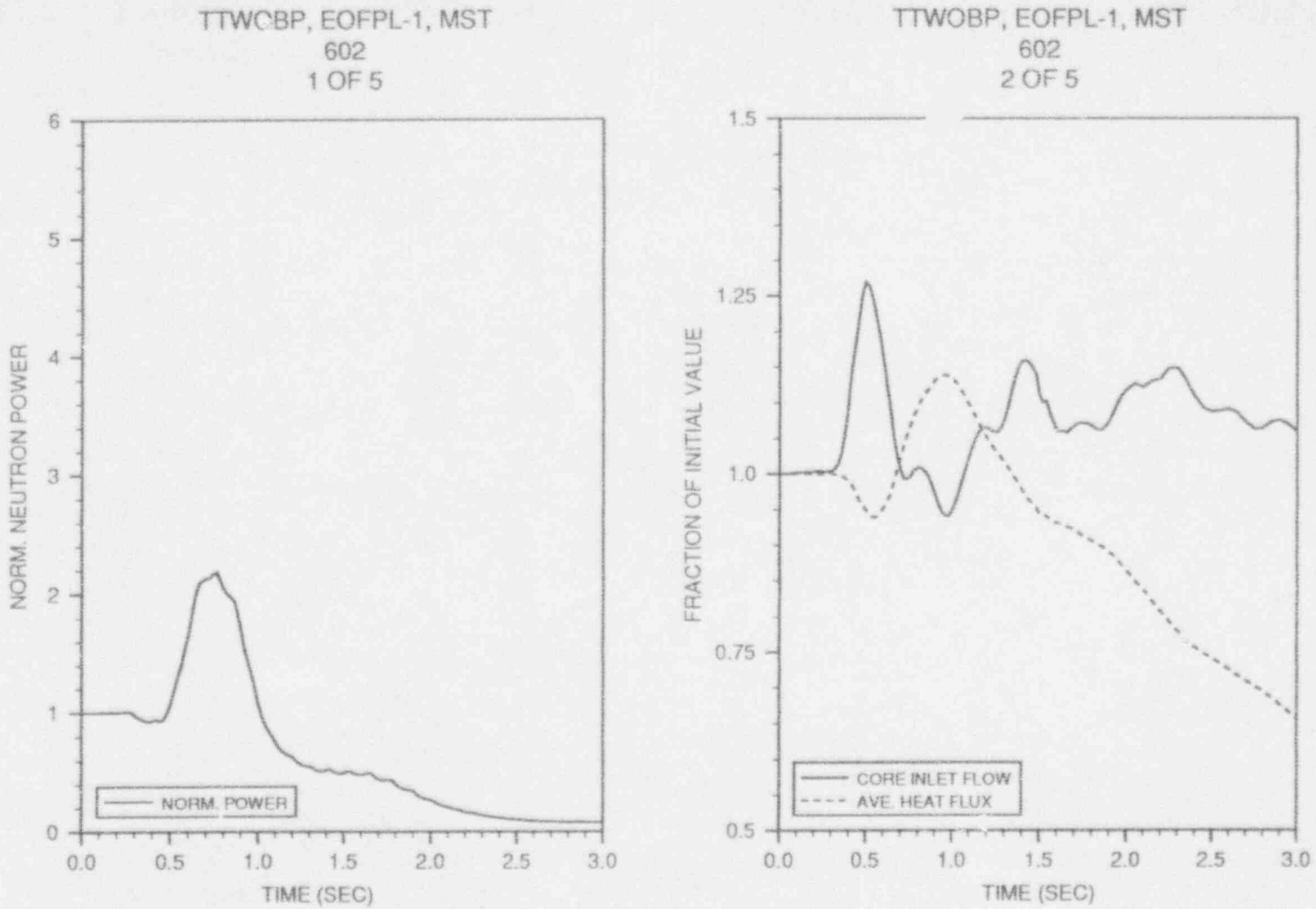

FIGURE 7.2.3

TURBINE TRIP WITHOUT BYPASS, EOFPL17-1000 MWD/ST
TRANSIENT RESPONSE VERSUS TIME, "MEASURED" SCRAM TIME

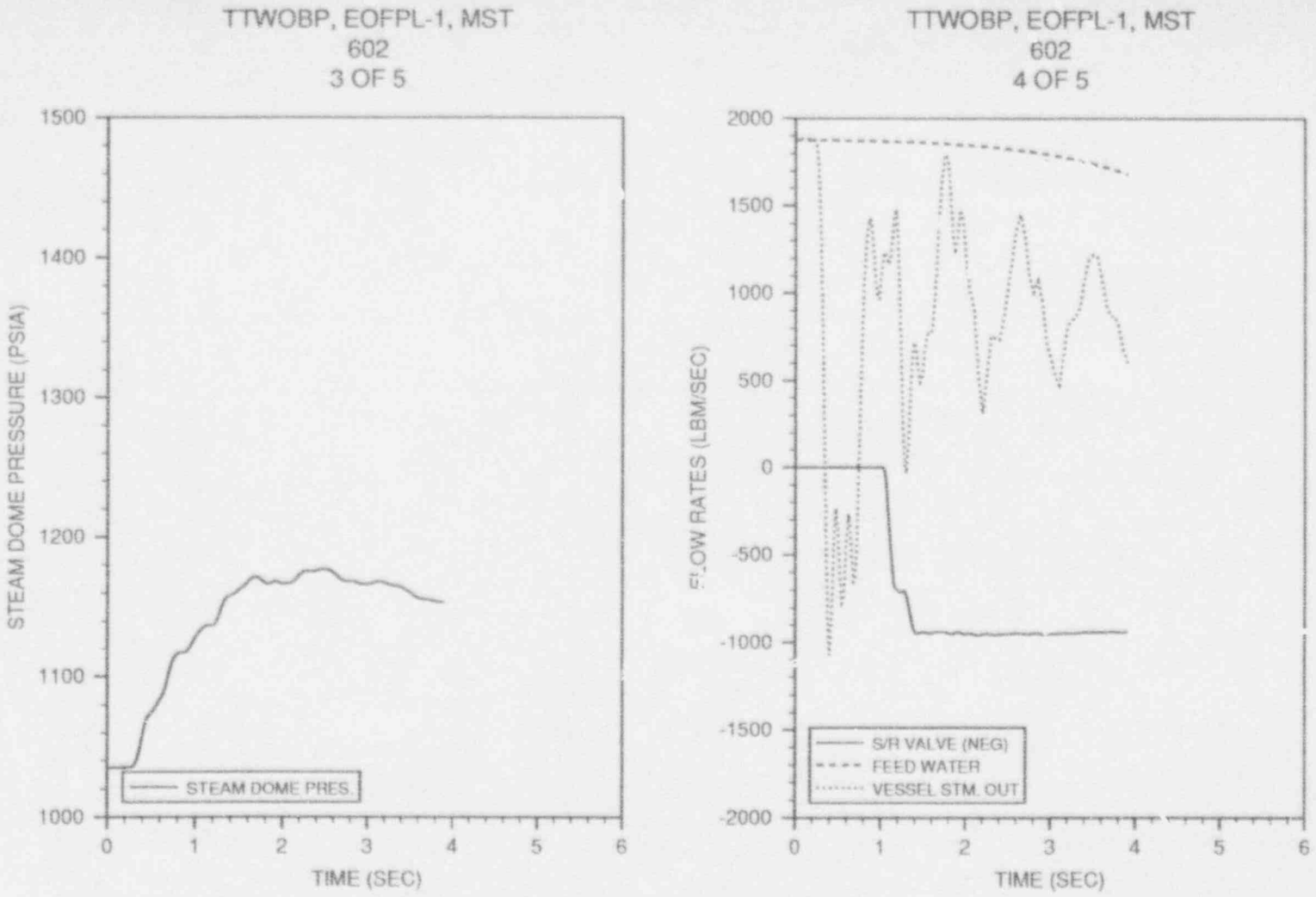

FIGURE 7.2.3
(Continued)

TURBINE TRIP WITHOUT BYPASS, EOFPL17-1000 MWD/ST
TRANSIENT RESPONSE VERSUS TIME, "MEASURED" SCRAM TIME

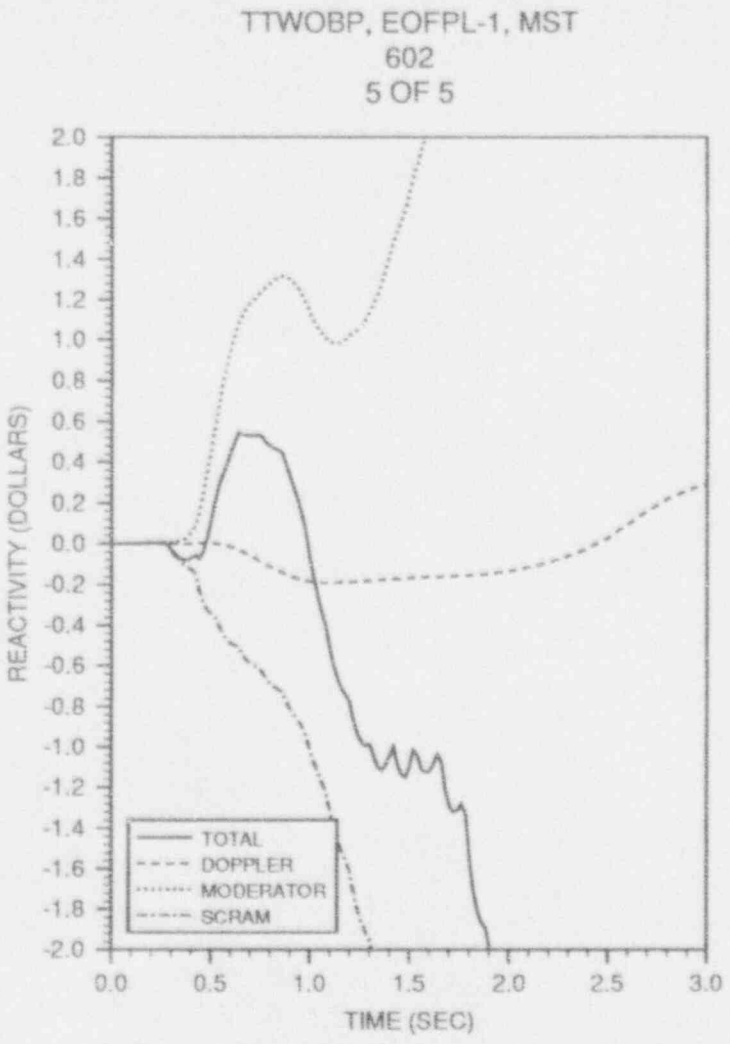

FIGURE 7.2.3
(Continued)

TURBINE TRIP WITHOUT BYPASS, EOFPL17-1000 MWD/ST
TRANSIENT RESPONSE VERSUS TIME, "MEASURED" SCRAM TIME

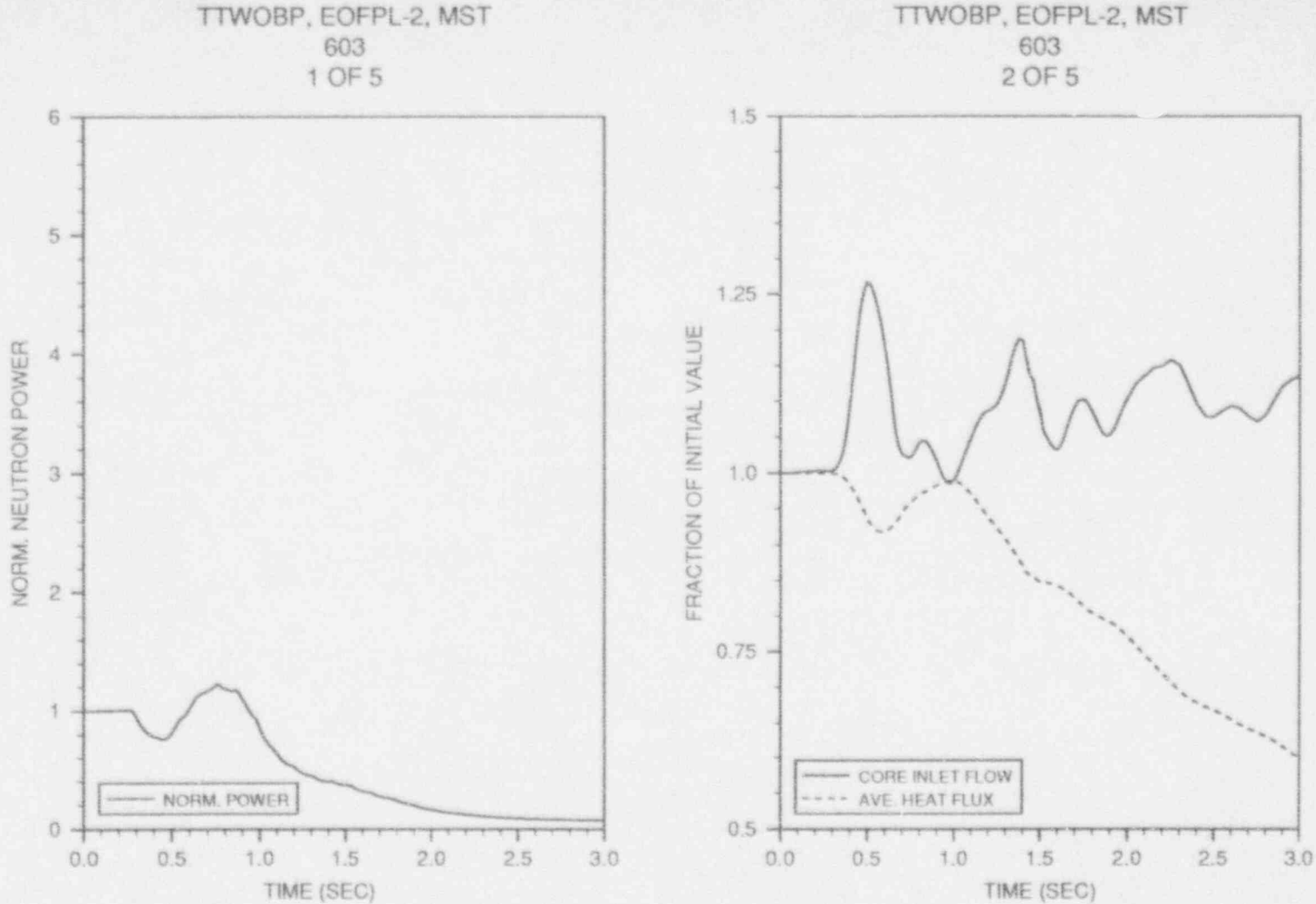

FIGURE 7.2.4

TURBINE TRIP WITHOUT BYPASS, EOFPL17-2000 MWD/ST
TRANSIENT RESPONSE VERSUS TIME, "MEASURED" SCRAM TIME

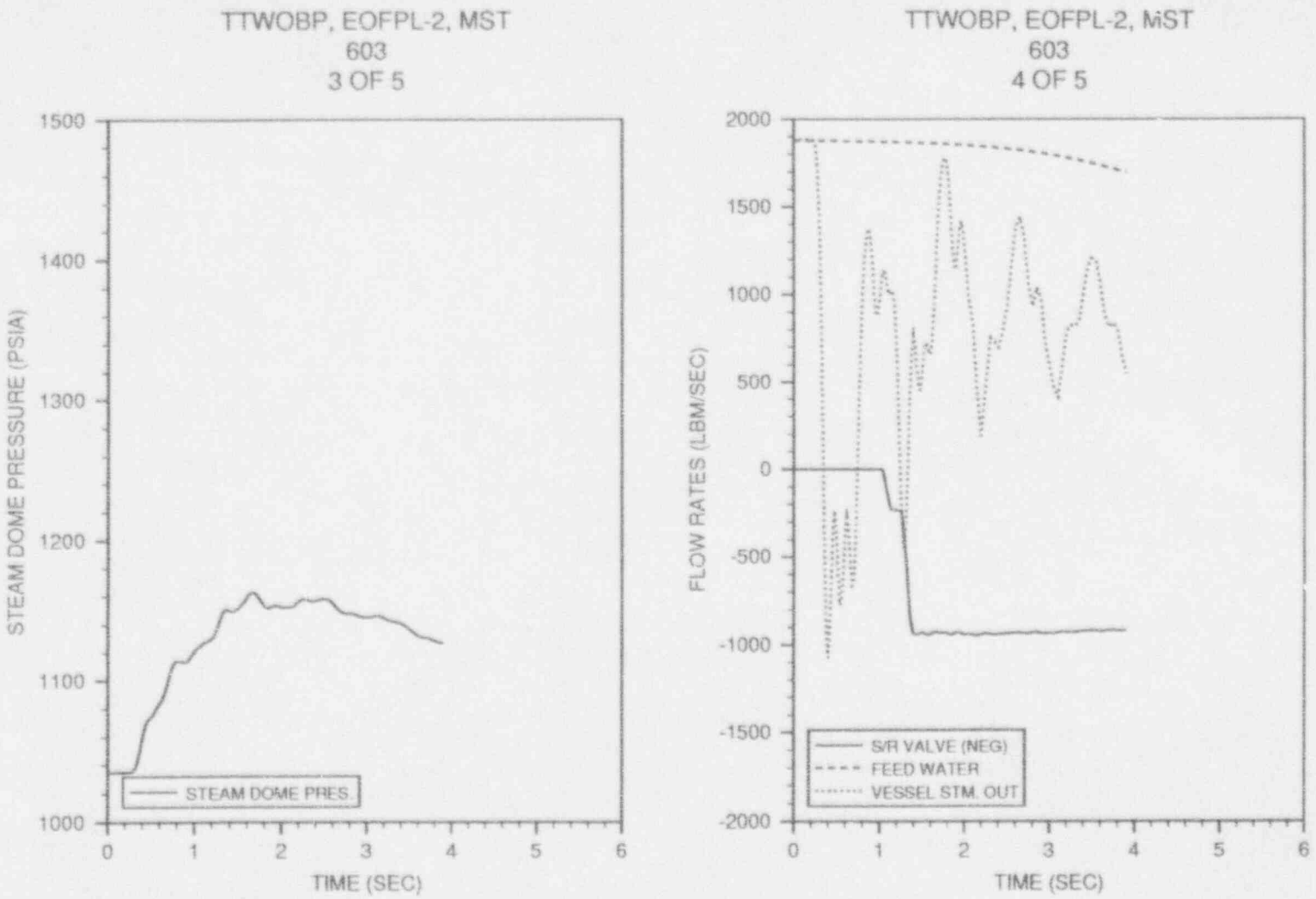

FIGURE 7.2.4
(Continued)

TURBINE TRIP WITHOUT BYPASS, EOFPL17-2000 MWD/ST
TRANSIENT RESPONSE VERSUS TIME, "MEASURED" SCRAM TIME

TTWOBP, EOFPL-2, MST
603
5 OF 5

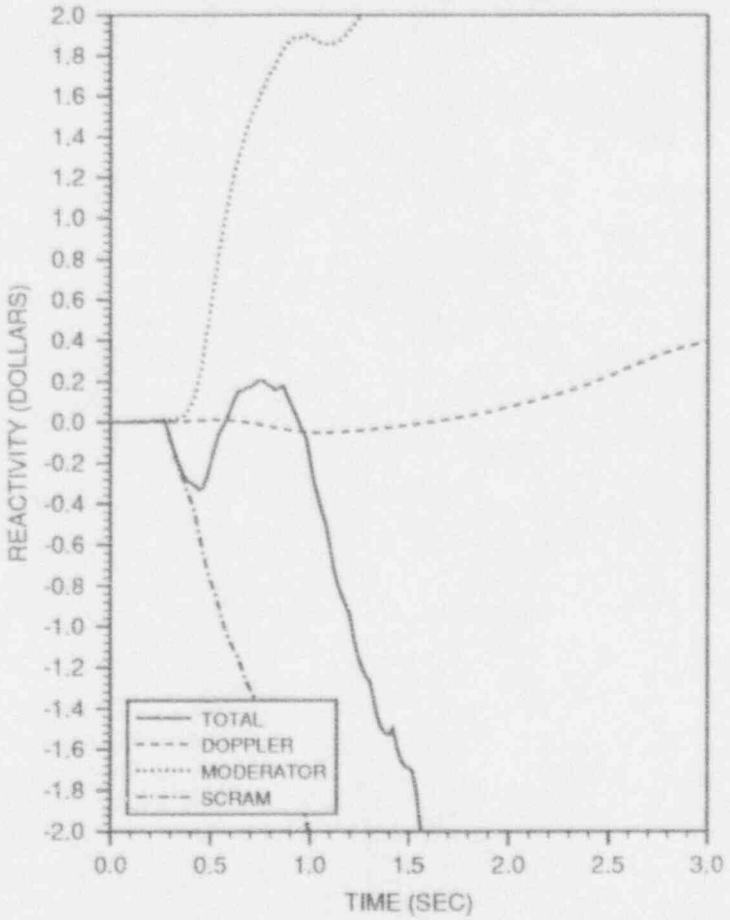

FIGURE 7.2.4
(Continued)

TURBINE TRIP WITHOUT BYPASS, EOFPL17-2000 MWD/ST
TRANSIENT RESPONSE VERSUS TIME, "MEASURED" SCRAM TIME

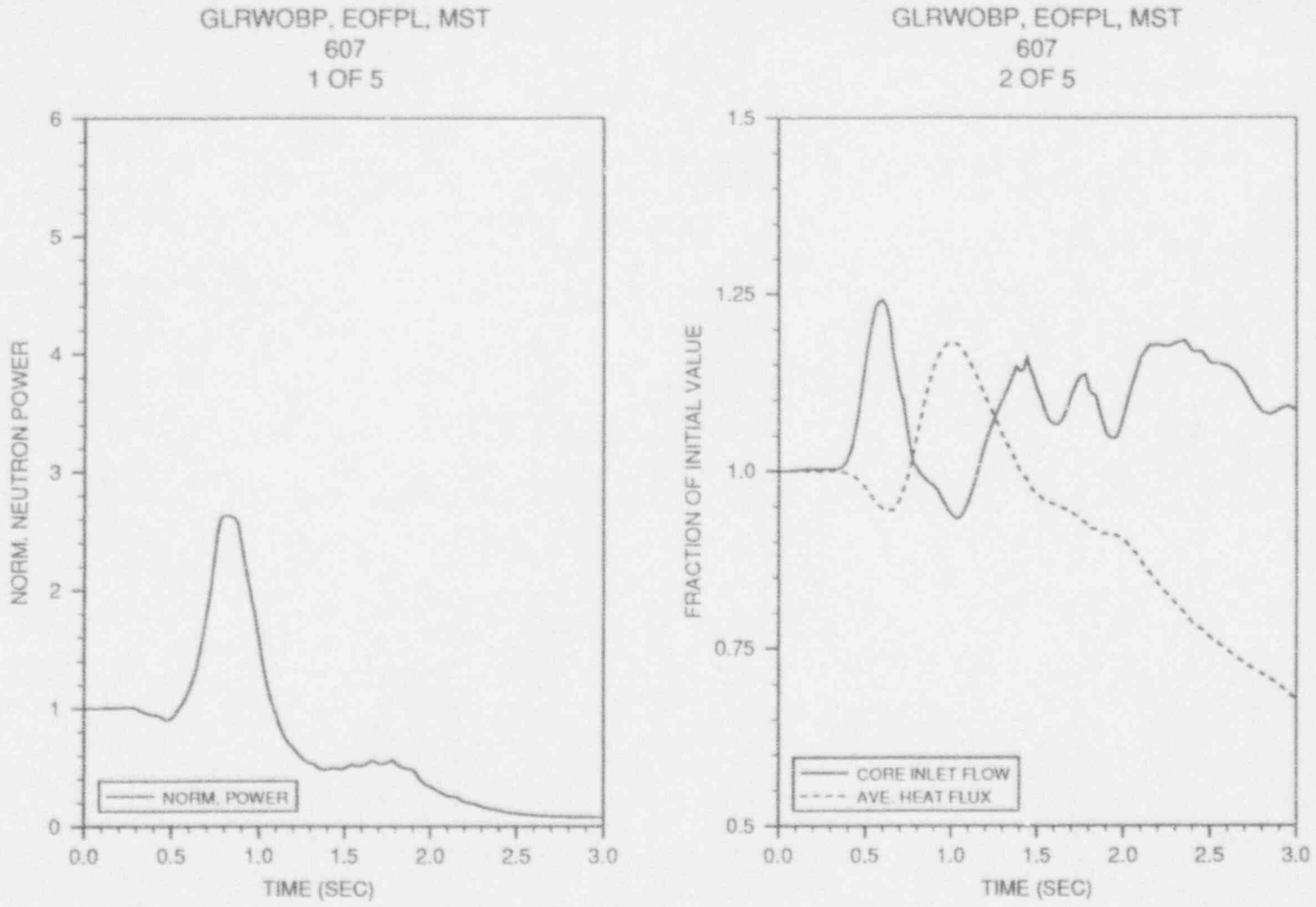

FIGURE 7.2.5

GENERATOR LOAD REJECTION WITHOUT BYPASS, EOFPL17
TRANSIENT RESPONSE VERSUS TIME, "MEASURED" SCRAM TIME

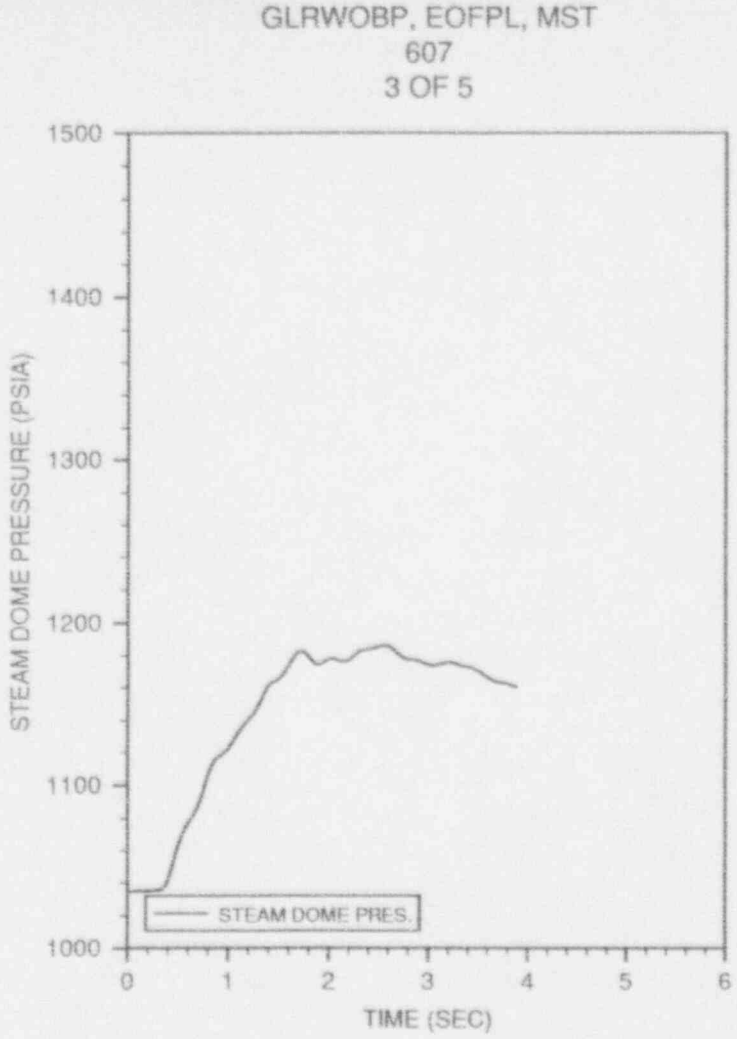

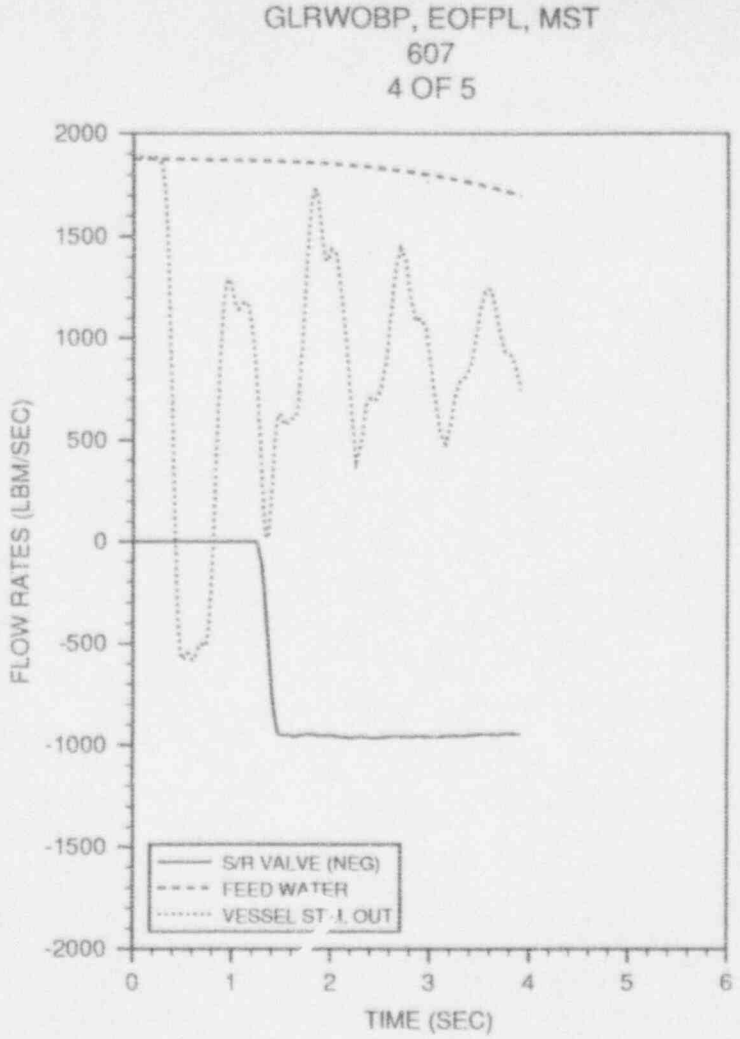

FIGURE 7.2.5
(Continued)

GENERATOR LOAD REJECTION WITHOUT BYPASS, EOFPL17
TRANSIENT RESPONSE VERSUS TIME, "MEASURED" SCRAM TIME

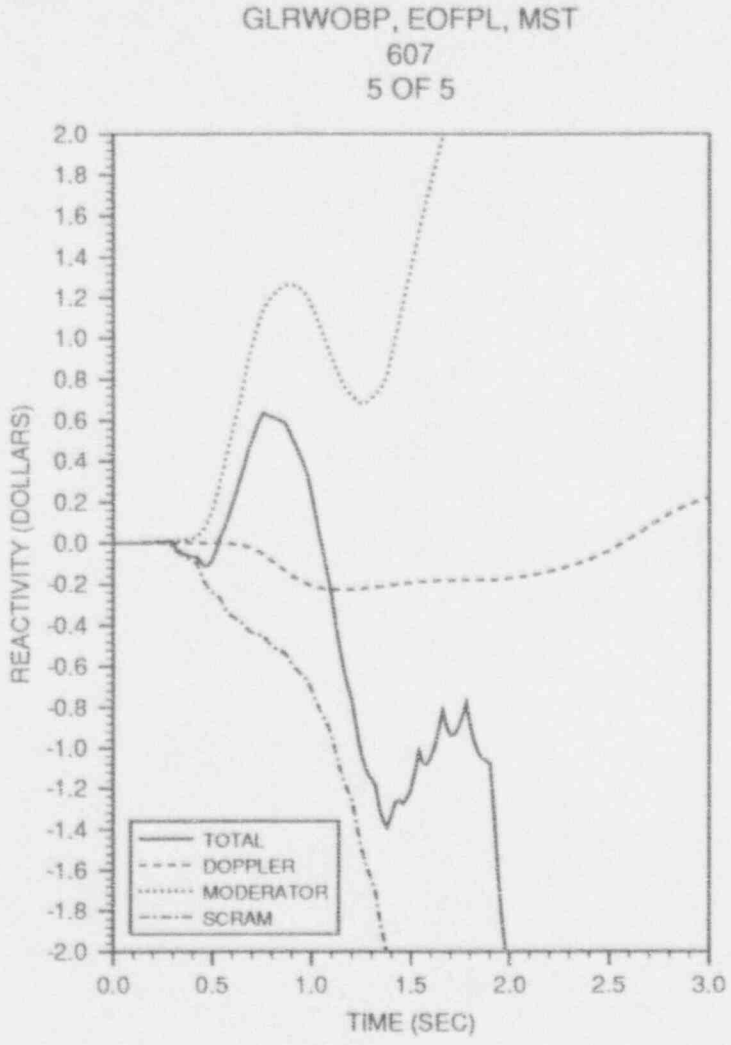

FIGURE 7.2.5
(Continued)

GENERATOR LOAD REJECTION WITHOUT BYPASS, EOFPL17
TRANSIENT RESPONSE VERSUS TIME, "MEASURED" SCRAM TIME

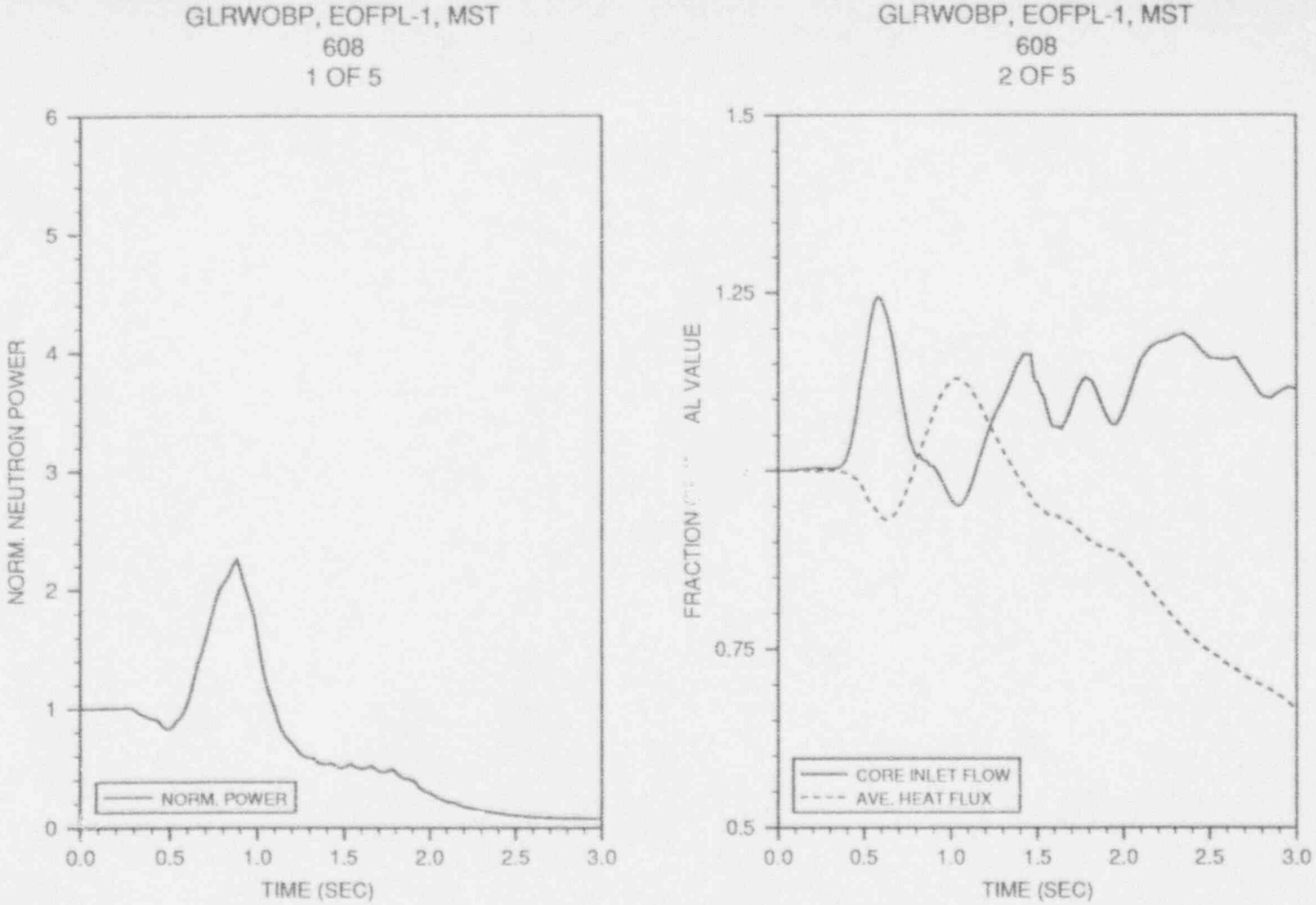

FIGURE 7.2.6

GENERATOR LOAD REJECTION WITHOUT BYPASS, EOFPL17-1000 MWD/ST
TRANSIENT RESPONSE VERSUS TIME, "MEASURED" SCRAM TIME

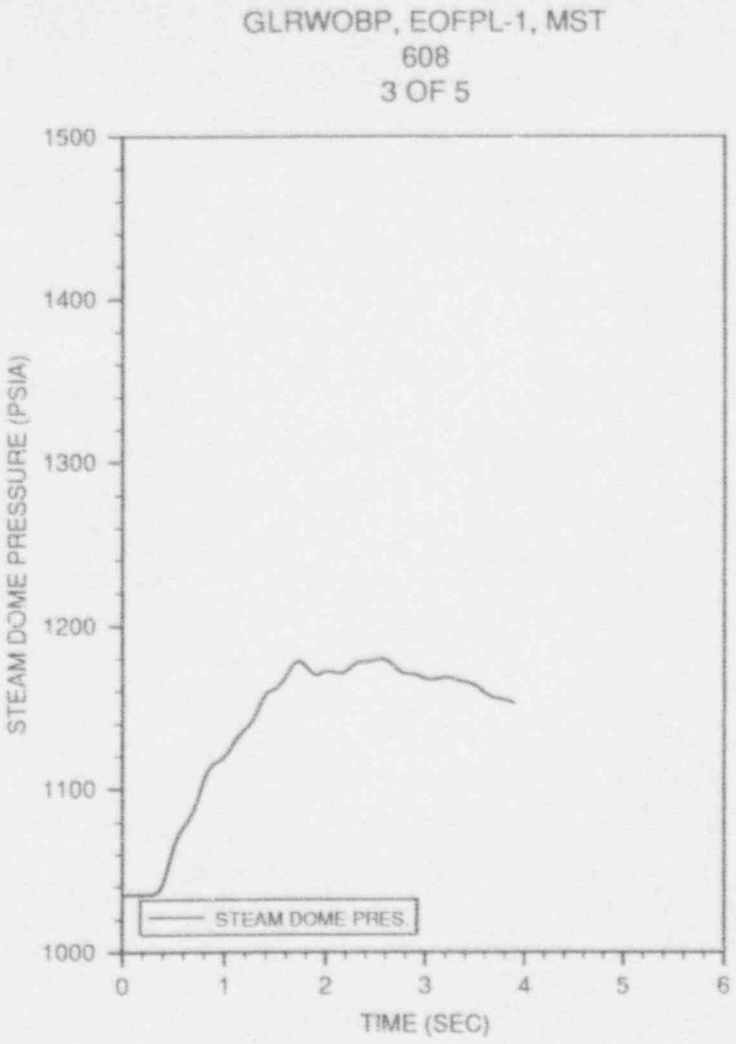

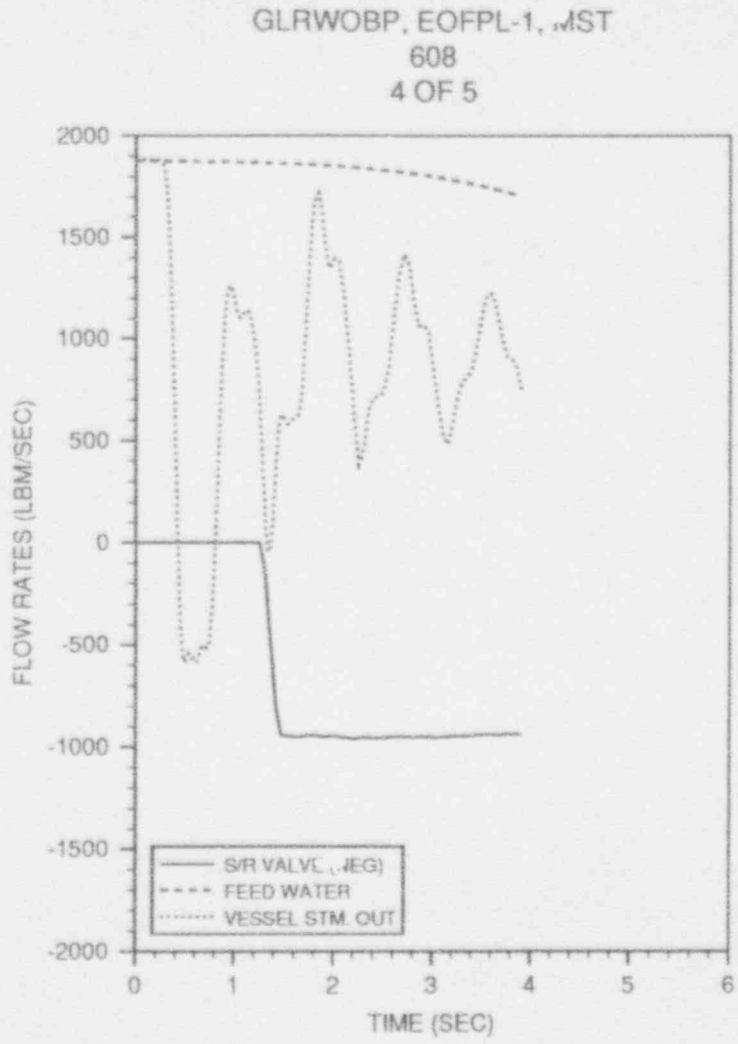

FIGURE 7.2.6
(Continued)

GENERATOR LOAD REJECTION WITHOUT BYPASS, EOFPL17-1000 MWD/ST
TRANSIENT RESPONSE VERSUS TIME, "MEASURED" SCRAM TIME

GLRWOBP, EOFPL-1, MST
608
5 OF 5

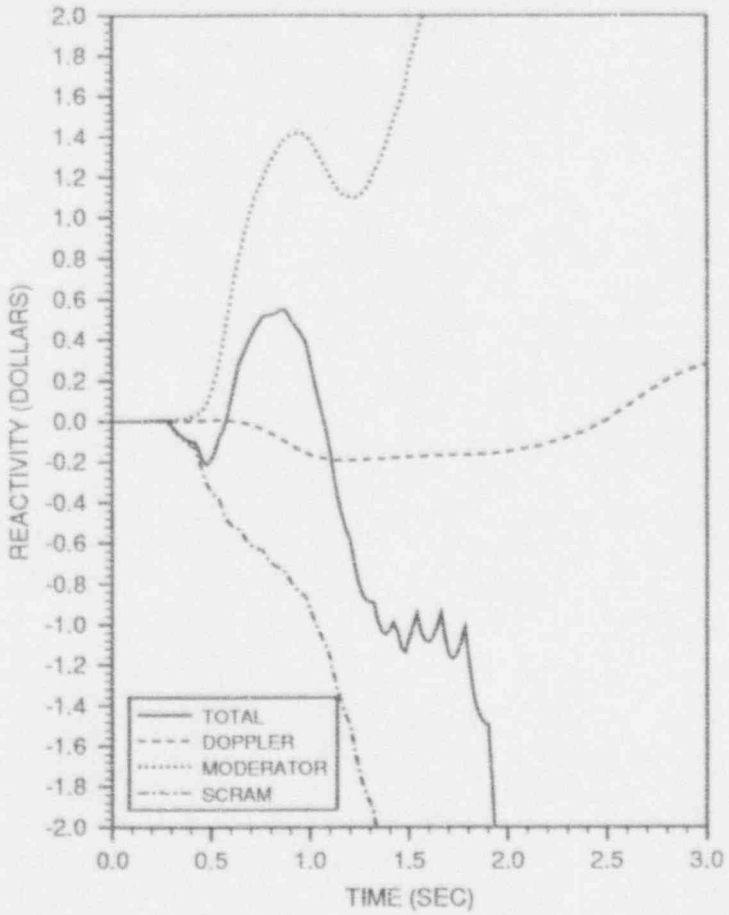

FIGURE 7.2.6
(Continued)

GENERATOR LOAD REJECTION WITHOUT BYPASS, EOFPL17-1000 MWD/ST
TRANSIENT RESPONSE VERSUS TIME, "MEASURED" SCRAM TIME

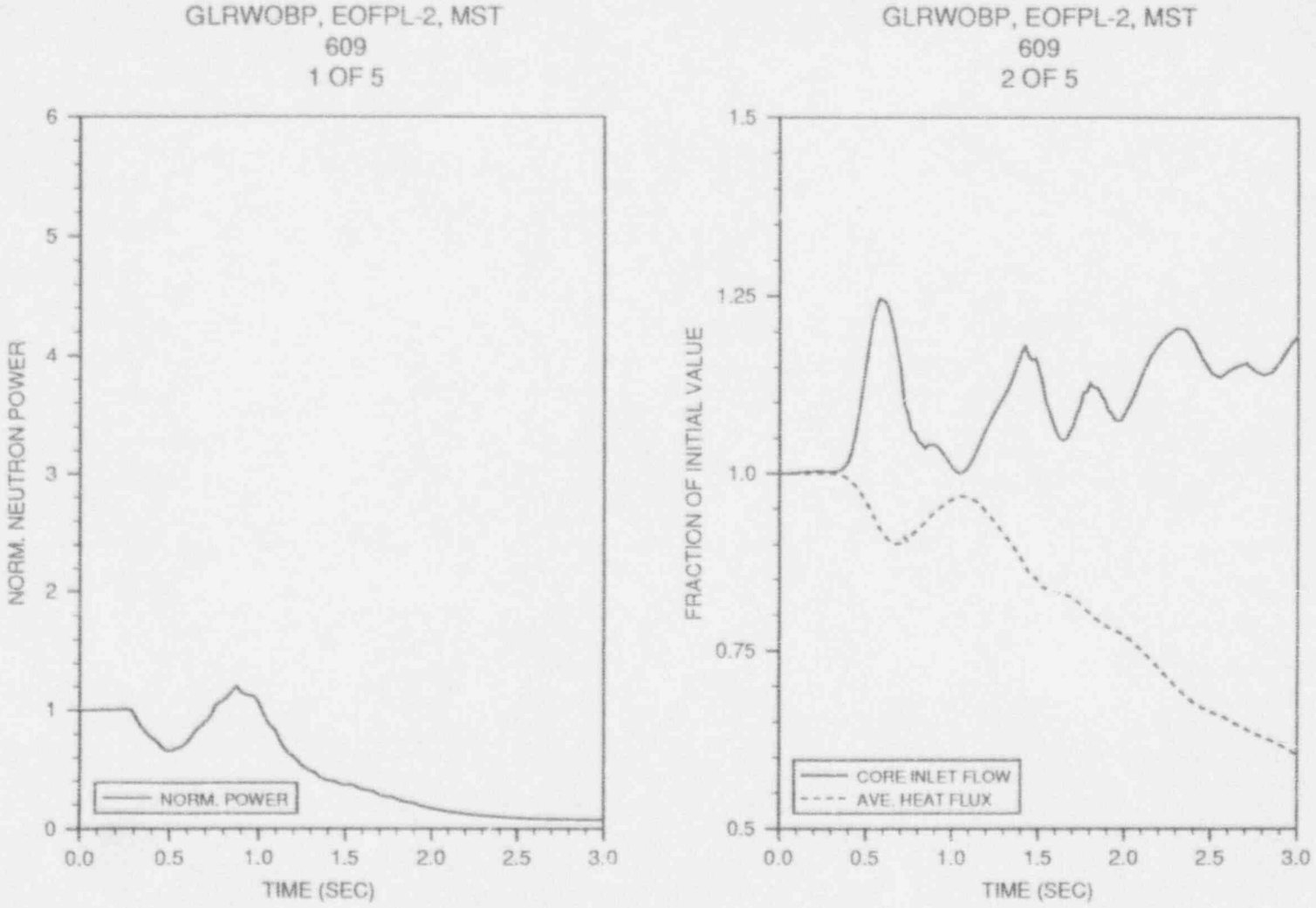

FIGURE 7.2.7

GENERATOR LOAD REJECTION WITHOUT BYPASS, EOFPL17-2000 MWD/ST
TRANSIENT RESPONSE VERSUS TIME, "MEASURED" SCRAM TIME

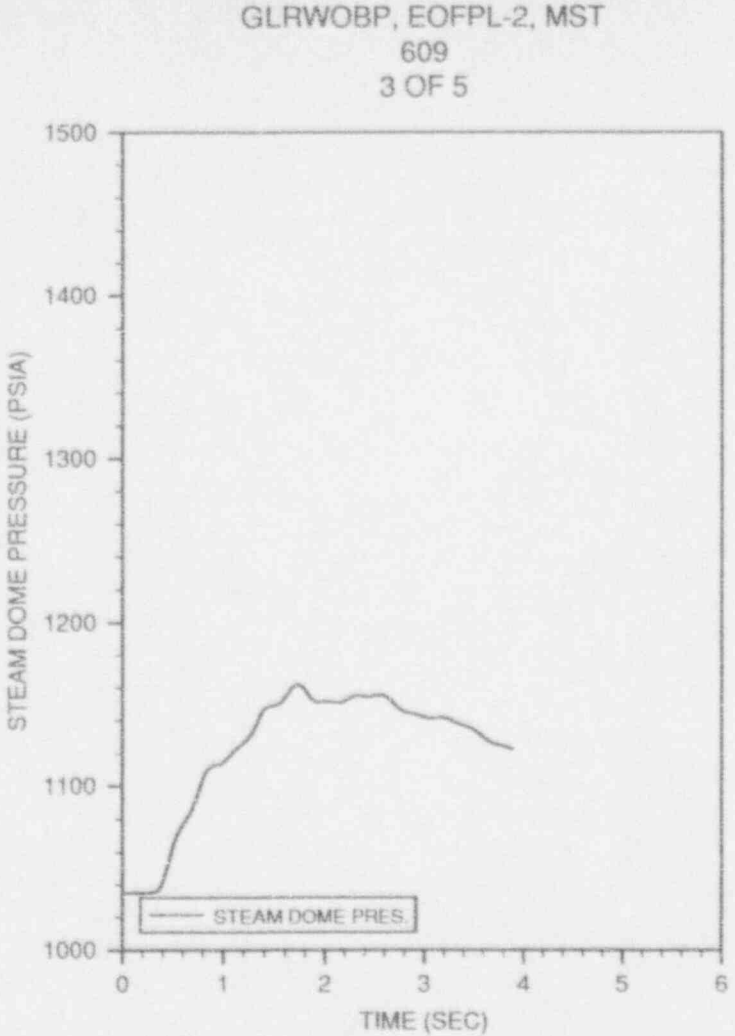

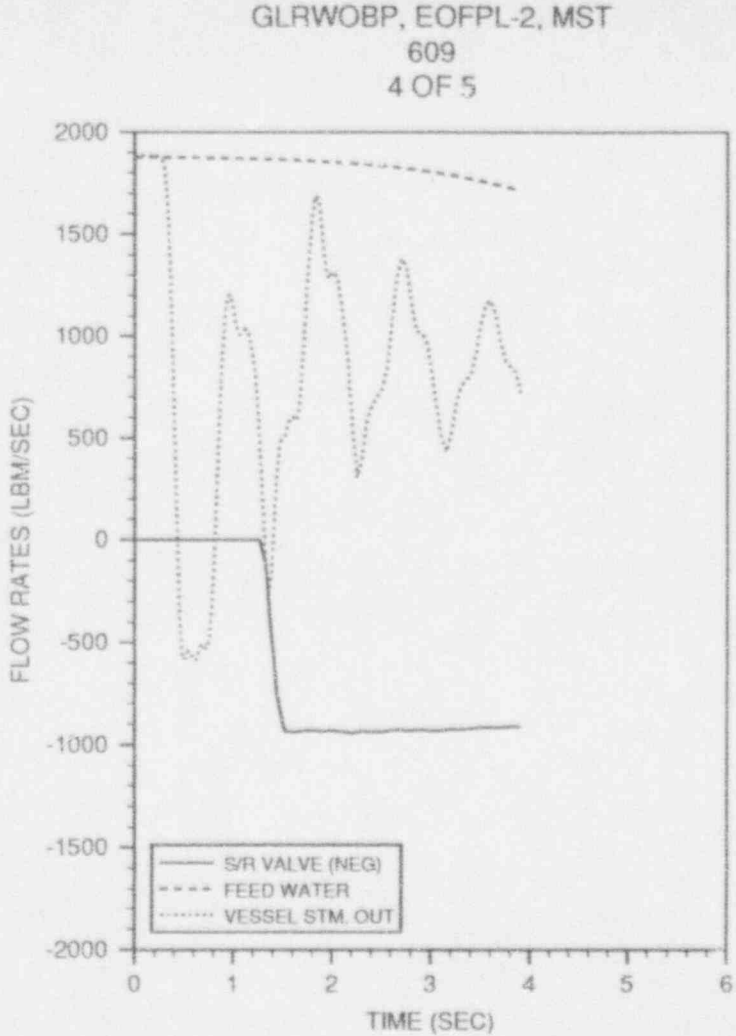

FIGURE 7.2.7
(Continued)

GENERATOR LOAD REJECTION WITHOUT BYPASS, EOFPL17-2000 MWD/ST
TRANSIENT RESPONSE VERSUS TIME, "MEASURED" SCRAM TIME

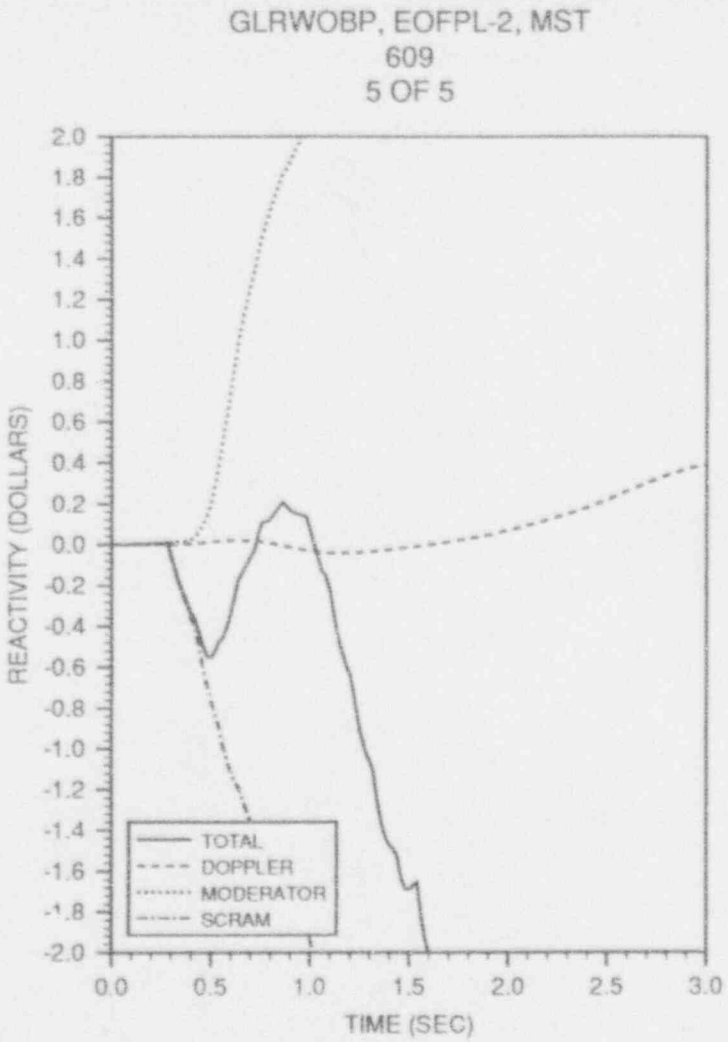

FIGURE 7.2.7
(Continued)

GENERATOR LOAD REJECTION WITHOUT BYPASS, EOFPL17-2000 MWD/ST
TRANSIENT RESPONSE VERSUS TIME, "MEASURED" SCRAM TIME

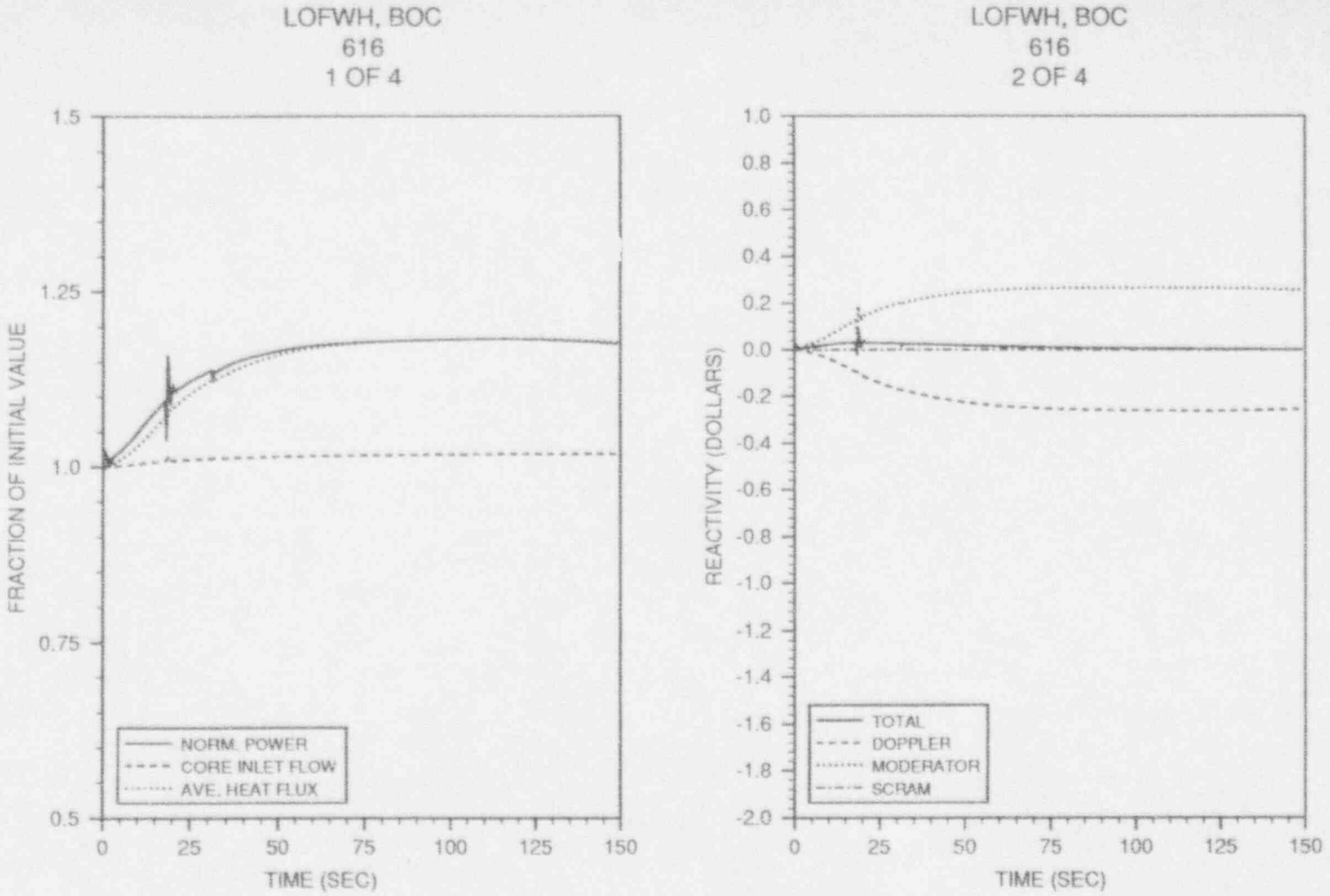

FIGURE 7.3.1

LOSS OF 100°F FEEDWATER HEATING, BOC17 (LIMITING CASE)
TRANSIENT RESPONSE VERSUS TIME

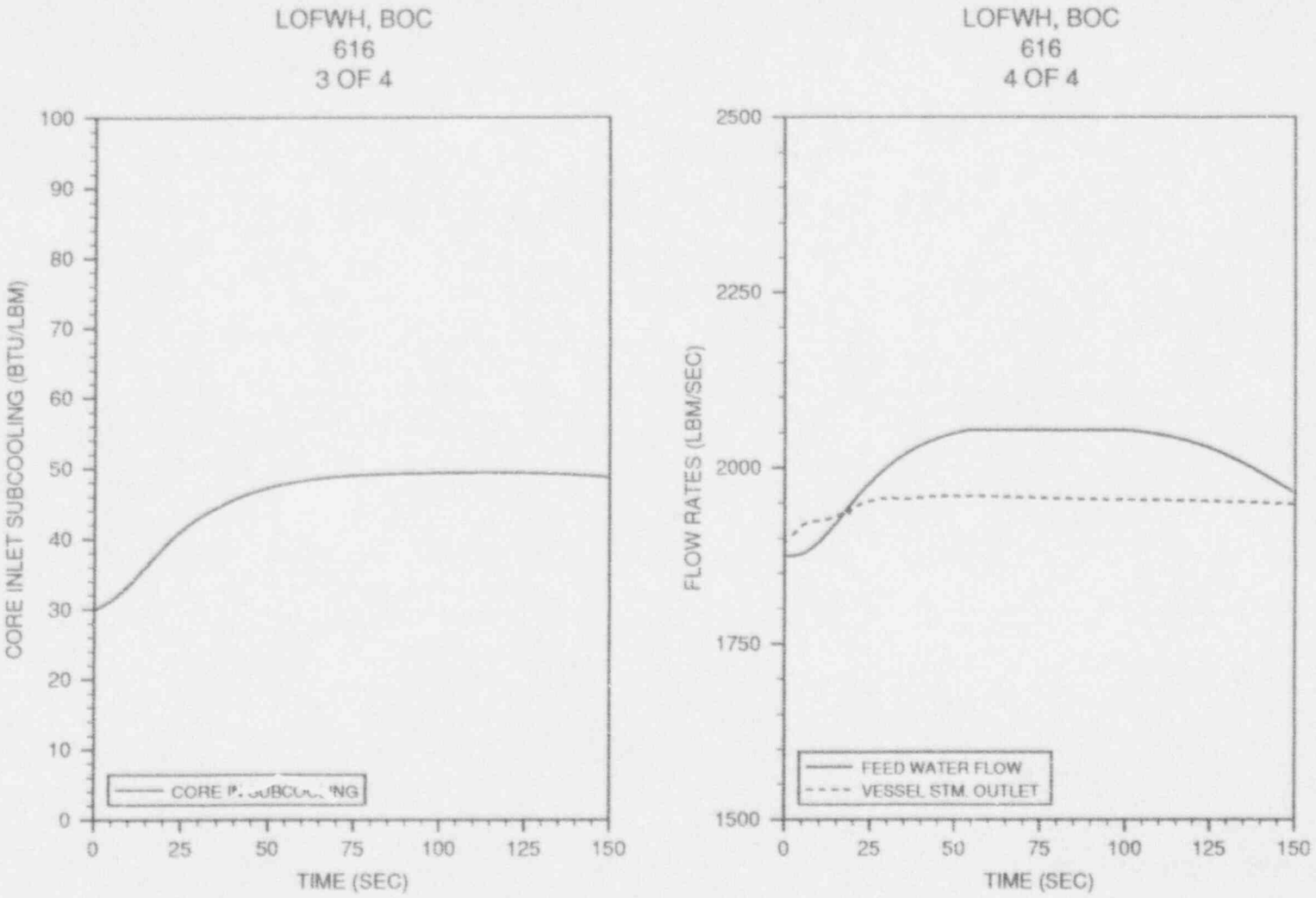

FIGURE 7.3.1
(Continued)

LOSS OF 100°F FEEDWATER HEATING, BOC17 (LIMITING CASE)
TRANSIENT RESPONSE VERSUS TIME

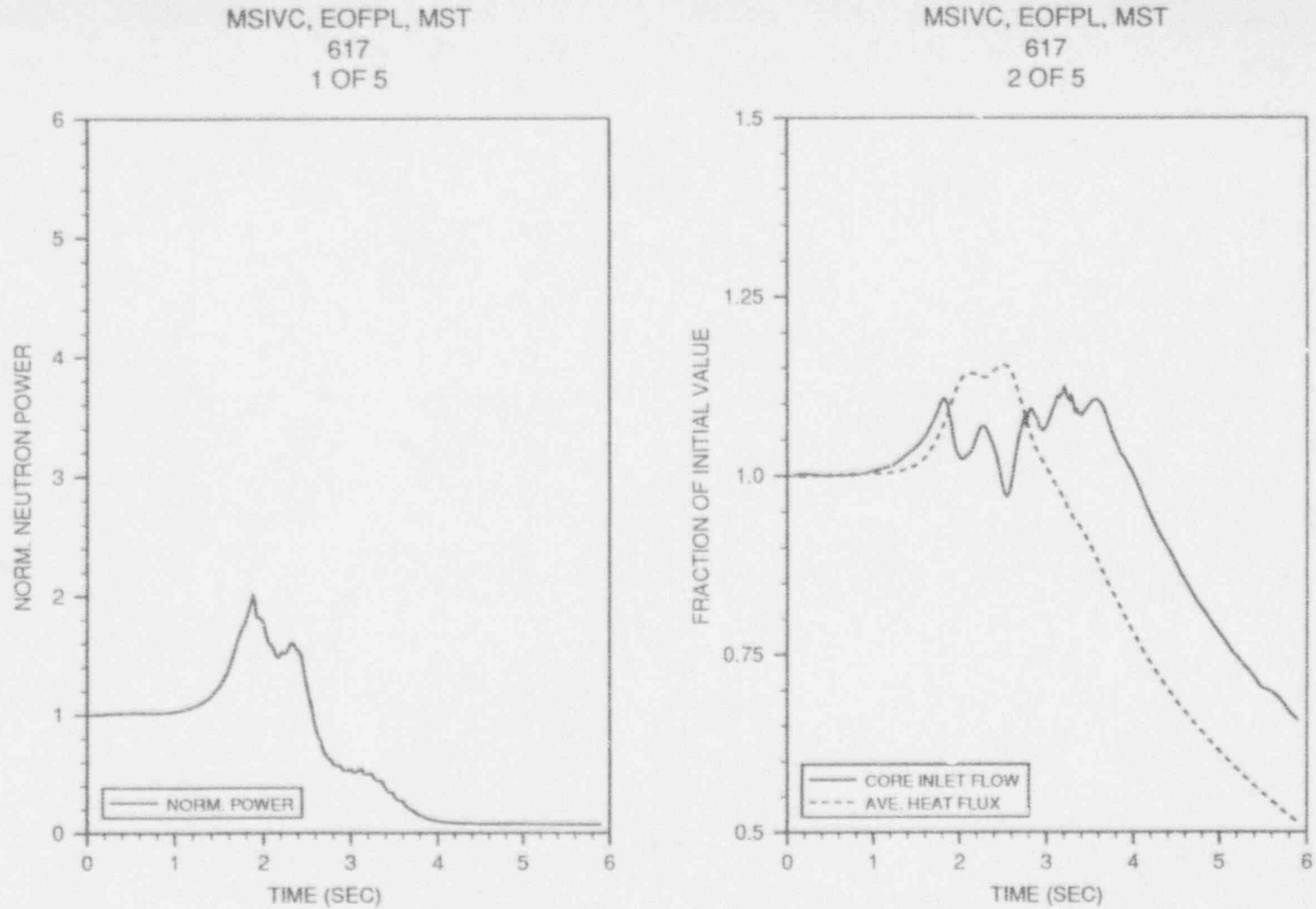

FIGURE 7.4.1

MSIV CLOSURE, FLUX SCRAM, EOFPL17
TRANSIENT RESPONSE VERSUS TIME, "MEASURED" SCRAM TIME

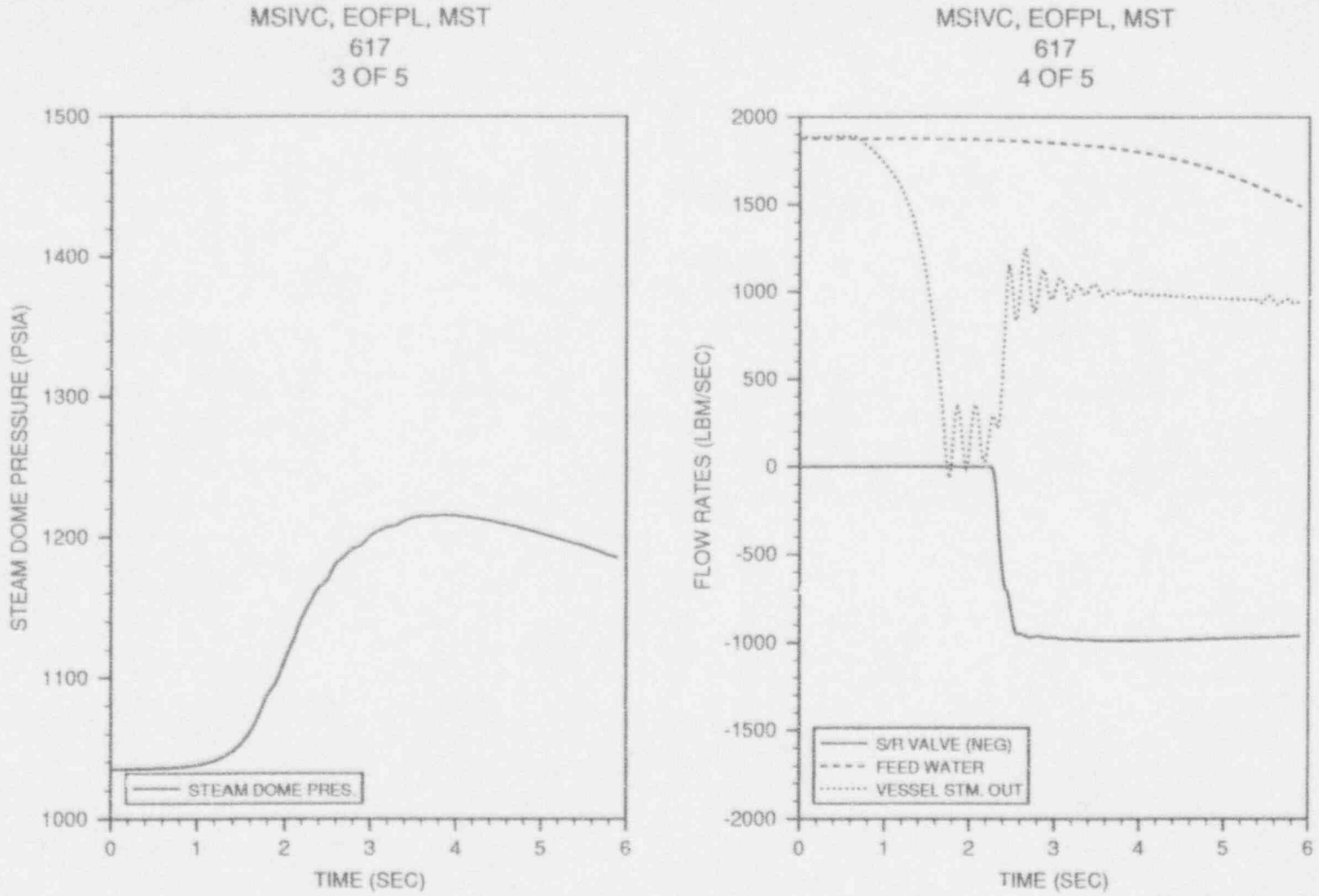

FIGURE 7.4.1
(Continued)

MSIV CLOSURE, FLUX SCRAM, EOFPL17
TRANSIENT RESPONSE VERSUS TIME, "MEASURED" SCRAM TIME

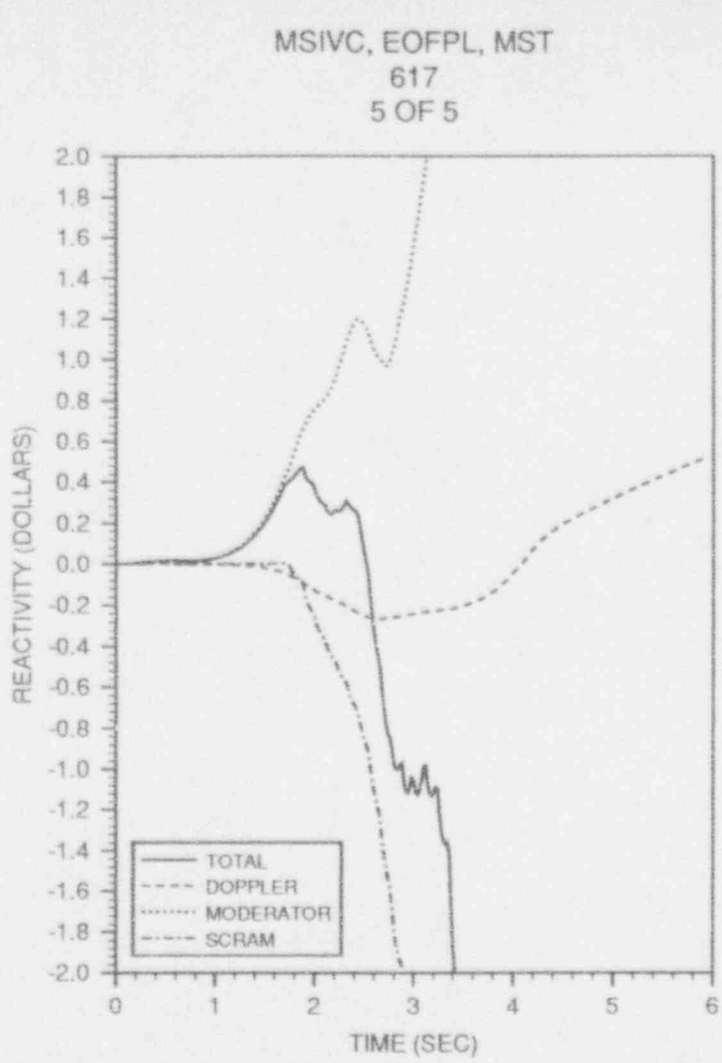

FIGURE 7.4.1
(Continued)

MSIV CLOSURE, FLUX SCRAM, EOFPL17
TRANSIENT RESPONSE VERSUS TIME, "MEASURED" SCRAM TIME

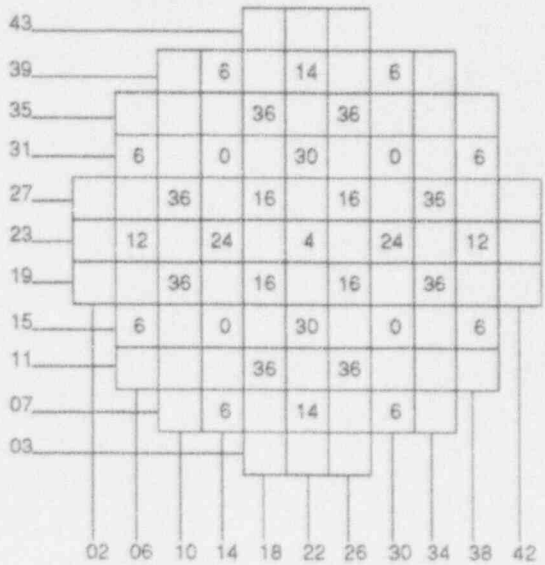

Core Thermal Power	=	1664 MW_{th}
Initial MCPR	=	1.302
Core Flow	=	48 Mlb/hr
RWE Control Rod	=	30-15
Core Exit Pressure	=	1042 psia
Zero Xenon		

TRANSIENT SUMMARY

RBM Setpoint	Rod Position at RBM Setpoint	ΔCPR	Transient MCPR Limit
104	12	0.14	1.21
105	14	0.18	1.25
106	14	0.18	1.25
107	16	0.23	1.30
108	18	0.27	1.34

FIGURE 7.5.1

REACTOR INITIAL CONDITIONS AND TRANSIENT SUMMARY FOR THE VY CYCLE 17 ROD WITHDRAWAL ERROR CASE 1

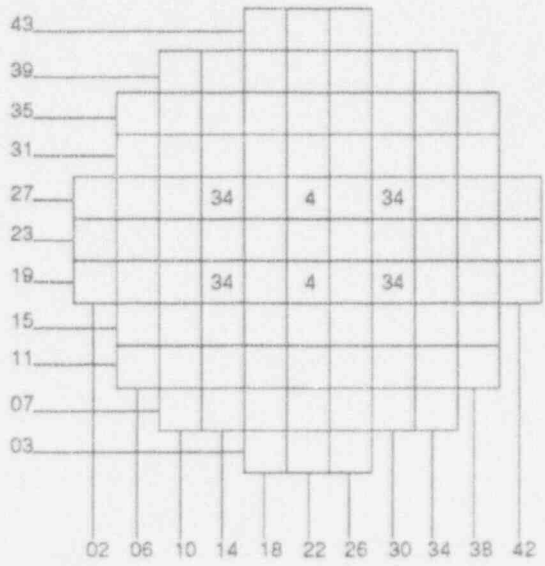

Core Thermal Power	=	1593 MW_{th}
Initial MCPR	=	1.528
Core Flow	=	46 Mlb/hr
RWE Control Rod	=	22-19
Core Exit Pressure	=	1032 psia
Equilibrium Xenon		

TRANSIENT SUMMARY

RBM Setpoint	Rod Position at RBM Setpoint	ΔCPR
104	12	0.10
105	14	0.11
106	16	0.14
107	22	0.19
108	26	0.22

FIGURE 7.5.2

REACTOR INITIAL CONDITIONS AND TRANSIENT SUMMARY FOR THE VY CYCLE 17 ROD WITHDRAWAL ERROR CASE 2

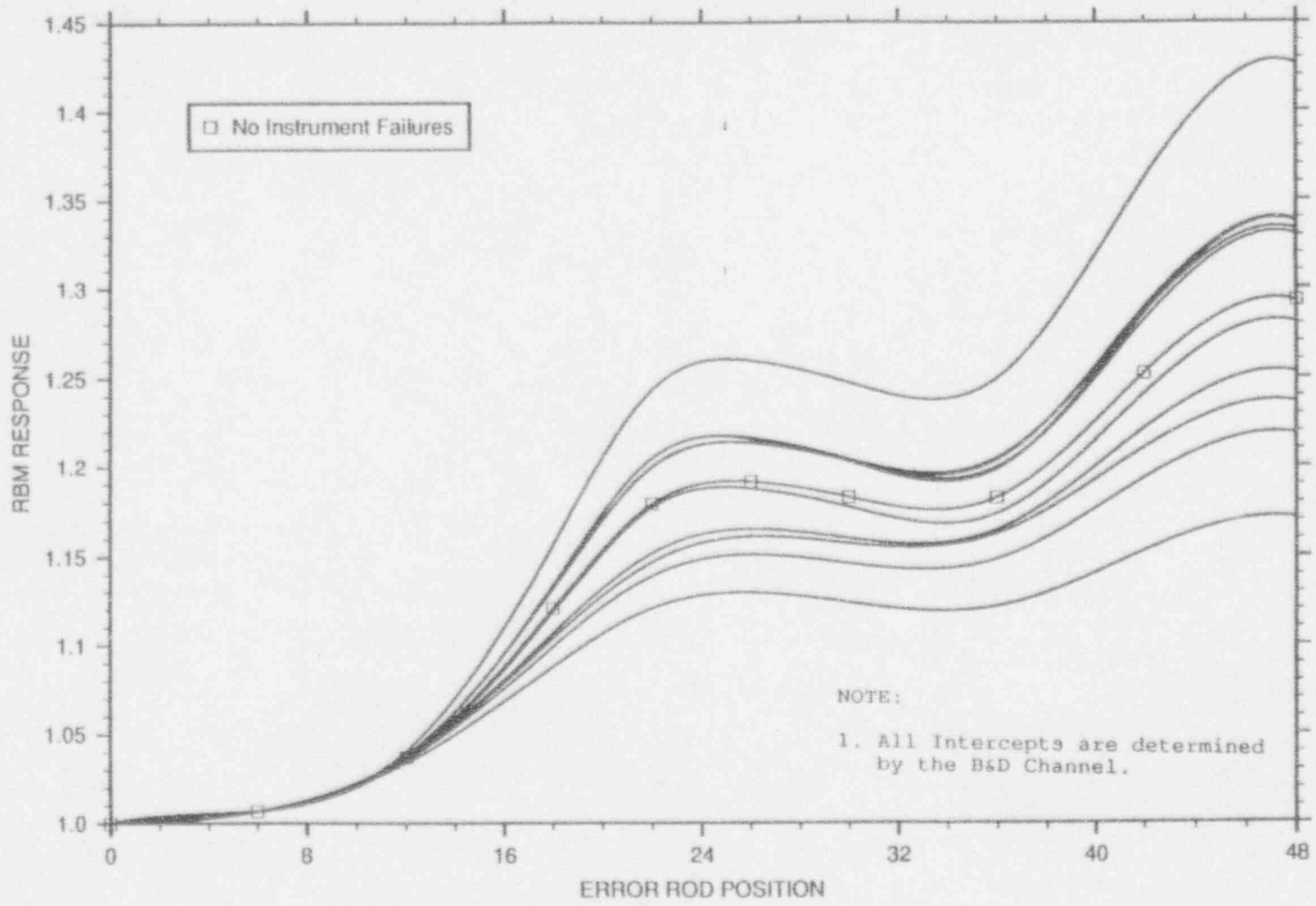

FIGURE 7.5.3

VY CYCLE 17 RWE CASE 1 - SETPOINT INTERCEPTS DETERMINED BY THE A AND C CHANNELS

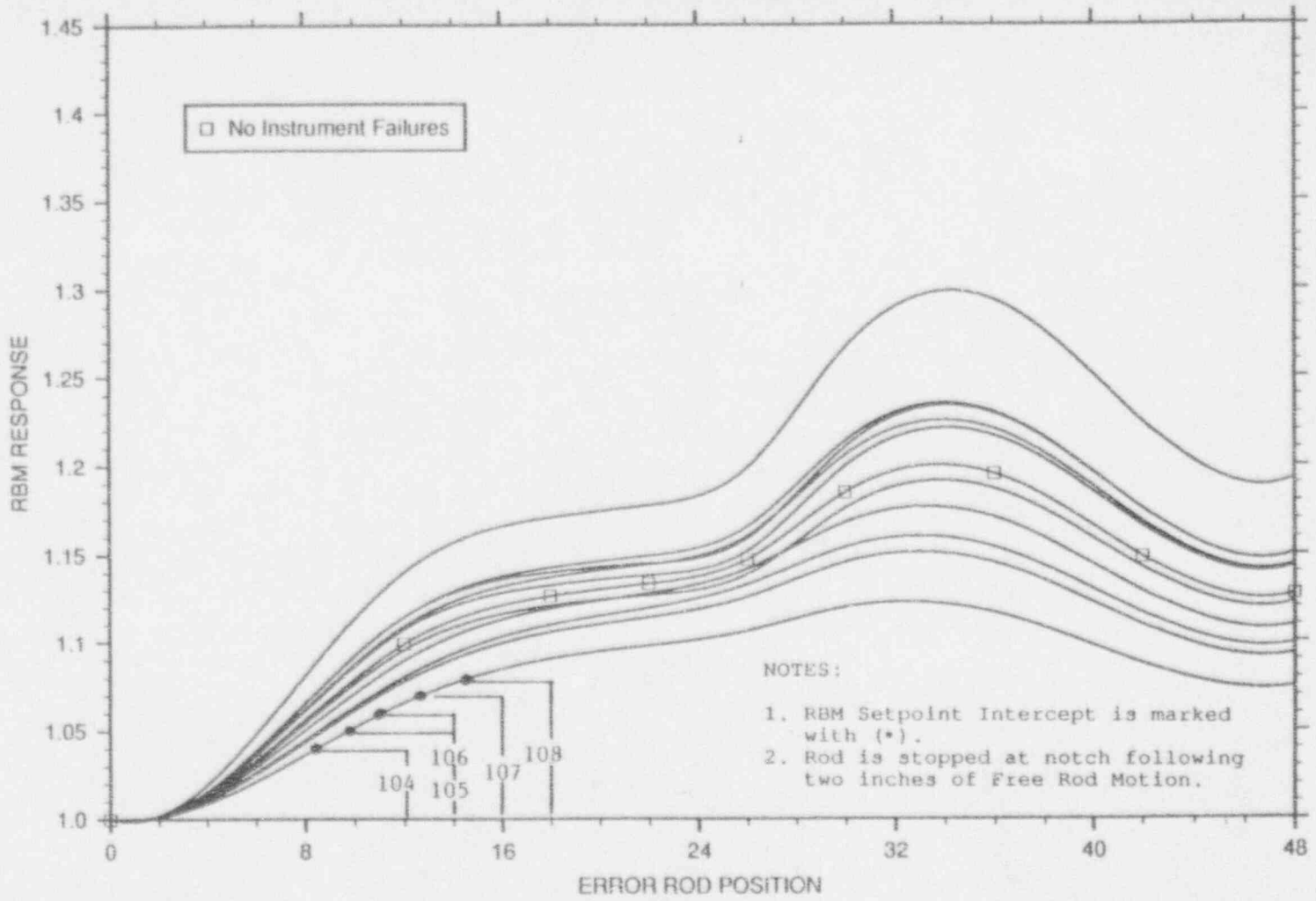

FIGURE 7.5.4

VY CYCLE 17 RWE CASE 1 - SETPOINT INTERCEPTS DETERMINED BY THE B AND D CHANNELS

8.0 DESIGN BASIS ACCIDENT ANALYSIS

8.1 Control Rod Drop Accident Results

The control rod sequences are a series of rod withdrawal and banked withdrawal instructions specifically designed to minimize the worths of individual control rods. The sequences are examined so that, in the event of the uncoupling and subsequent free fall of the rod, the incremental rod worth is acceptable. Incremental rod worth refers to the fact that rods beyond Group 2 are banked out of the core and can only fall the increment from full-in to the rod drive withdrawal position. Acceptable worth is one which produces a maximum fuel enthalpy less than 280 calories per gram.

Some out-of-sequence control rods could accrue potentially high worths. However, the Rod Worth Minimizer (RWM) will prevent withdrawing an out-of-sequence rod, if accidentally selected. The RWM is functionally tested before each startup.

The sequence in the RWM will take the plant from All Rods In (ARI) to well above 20% core thermal power. Above 20% power even multiple operator errors will not create a potential rod drop situation above 280 calories per gram[29],[30],[31]. Below 20% power, however, the sequences must be examined for incremental rod worth. This is done throughout the cycle using the full core, xenon-free SIMULATE-3 model.

Both the A and B sequences were examined at various exposures throughout the cycle. For startup, the rods are grouped, as shown in Figures 8.1.1 and 8.1.2, and are pulled in numerical order. All the rods in one group are pulled out before the pulling of the next group begins. The rods in the first two groups are individually pulled from full-in to full-out. Beyond Group 2, the rods are banked out using procedures[32],[33] which reduce the rod incremental worths.

The potentially high worths that occur in pulling the rods in Group 1 are ignored because the reactor is subcritical in Group 1.

Therefore, if a rod drops from any configuration in the first group, its excess reactivity contribution to the Rod Drop Accident (RDA) is zero. Successive reloads of axially zoned fuel have extended this subcriticality situation to the second group as well.

The second group of rods was examined using the following analysis method[34]. Both the A and B sequences were examined. It was found that the highest worth rod was the first rod in the second group. Any of the first four rod arrays, shown in Figures 8.1.1 and 8.1.2, may be designated as the first group pulled. However, a specific second group must follow as Table 8.1.1 illustrates. For added conservatism, each of the high worth rods in the second group were checked; i.e., one at a time, they were assigned to be the first rod pulled. This assures that in any sequence the actual worths will always be less than those calculated here.

Only that portion of the control rod worth above the SIMULATE-3 cold critical eigenvalue contributes to the rod drop accident. For conservatism, "critical" was defined as the SIMULATE-3 average cold critical K_{eff} minus 1% ΔK (reactivity anomaly criteria). The results of the Group 2 calculations, as presented in Table 8.1.2, fit under the bounding analysis of References 29 through 31.

Beyond Group 2, the rods are banked out of the core. This generally limits the incremental worth of a single rod drop; however, virtually all of the pre-drop cases in Group 3 are critical. Therefore, the entire dropped rod worth contributes toward the RDA excess reactivity insertion. The method used to evaluate Group 3 involved pulling Groups 1 and 2 out and banking Group 3 to varying positions. The types of cases examined included:

1. Banked positions 04, 08, 12, and 48 (full-out).

2. Group 3 rods pulled out of sequence, creating high flux regions.

3. Xenon-free conditions, both cold moderator and "standby"

(i.e., 1020 psia).

4. Group 3 rods dropping from 00 (full-in) to the appropriate banked position.

5. Stuck rods from previously pulled Group 1 or 2 dropping from 00 to 48.

The highest worth results from the Group 3 analysis fit under the Group 2 results, presented in Table 8.1.2.

8.2 Loss-of-Coolant Accident Analysis

The results of the complete evaluation of the loss-of-coolant accident (LOCA) for Vermont Yankee[35] provides the required support for the operation of the Reload Cycle. The LOCA analysis, performed in accordance with 10CFR50 Appendix K and the Safety Evaluation Reports[36][37], demonstrates that Vermont Yankee, operating within the assumed conditions, complies with the LOCA limits specified in 10CFR50.

The assumed initial conditions are listed in Table 8.2.1. Reference 35 provides a more detailed listing of the input assumptions. FROSSTEY-2, using the USNRC approved methodology[11], provided the fuel related initial conditions for the RELAP5YA calculations. The initial conditions were provided for the three core power regions and the peak high power rod at several exposures and axial power shapes. The initial conditions were fuel volume average temperature, internal rod pressure, gap inventory, and fuel and cladding geometries. The fuel volume average temperature was calculated at the upper 95/95 limit. The impact of the Gd_2O_3 on initial volume average temperature and material properties was included.

The LOCA analysis using RELAP5YA assured the licensing requirements were met by analyzing a combination of break size, break location, and single failure conditions. The break sizes range from

0.05 ft^2 to 7.28 ft^2. Five break locations were analyzed: main steam line, core spray line, feedwater line, recirculation loop suction and recirculation loop discharge. Five possible single failures were evaluated: low pressure coolant injection valve, high pressure coolant injection, DC power supply, diesel generator and one automatic depressurization system valve.

The analysis results showed that the limiting location was at the recirculation pump discharge. Figure 8.2.1 shows the peak cladding temperature as a function of break size for this location. The limiting case is the 0.6 ft^2 break size with one LPCI and one LPCS available. This corresponds to a single failure of one DC power supply. The analysis also assumed loss of offsite power concurrent with accident initiation. Overall, the calculated peak clad temperatures are below the 2200°F limit of 10CFR 50.46. The analysis also shows compliance with the other 10CFR 50.46 limits: total cladding oxidation at the peak location is less than 17%; hydrogen generated in the core is less than 1%; and the core retains a coolable geometry with no clad rupture.

During the cycle, Vermont Yankee can adjust the core flow to account for reactivity changes rather than using the control rods. During this type of operation, core flow may be as low as 87% while at 100% power. To ensure the safety analysis bounds these conditions, the LOCA analysis is analyzed at 1698 MW_{th} power and 87% flow. The results showed that the 100% flow case bounded the low flow case.

The analysis shows that the MAPLHGR limits are not limited by a LOCA. Therefore, the MAPLHGR limits are set based on the mechanical analysis of the bundle from Reference 18 and are provided in Appendix A for all the fuel types in the Reload Cycle, as a function of average planar exposure. Only the limiting MAPLHGR limits for the zoned fuel are provided in Appendix A. However, MAPLHGR limits exist for each lattice type and are specified in the process computer.

8.3 Refueling Accident Results

If any assembly is damaged during refueling, then a fraction of the fission product inventory could be released to the environment. The source term for the refueling accident is the maximum gap activity within any bundle. The source term includes contributions from both noble gases and iodines. The calculation of maximum gap activity is based on the MAPLHGRs, the maximum operating fuel centerline temperatures, and maximum bundle burnup.

The fuel rod gap activity, internal pressure and centerline temperature for the Reload Cycle are bounded by the values used in Section 14.9 of the FSAR[38].

TABLE 8.1.1

CONTROL ROD DROP ANALYSIS - ROD ARRAY PULL ORDER

The order in which rod arrays are pulled is specific once the choice of the first group is made.

First Group Pulled Is:	Second Group Pulled Must Be:	Successive Group Is Banked Out
Array 1	Array 2	Arrays 3 or 4
Array 2	Array 1	Arrays 3 or 4
Array 3	Array 4	Arrays 1 or 2
Array 4	Array 3	Arrays 1 or 2

TABLE 8.1.2

VY CYCLE 17 CONTROL ROD DROP ANALYSIS RESULTS

Maximum Incremental Rod Worth Calculated Cold, Xenon-Free	0.77% ΔK
Bounding Analysis Worth for Enthalpy Less than 280 Calories per Gram [29],[30],[31]	1.30% ΔK

TABLE 8.2.1

LOCA ANALYSIS ASSUMPTIONS

Core Thermal Power (MW_{th})	1698.3
Total Core Flow ($10^6 lb_m/hr$)	48.0
Reactor Vessel Pressure (psia)	1067.0
Recirculation Loop Flow ($10^6 lb_m/hr$) - Each Loop	12.3
Feedwater Flow ($10^6 lb_m/hr$)	6.93
Water Level Above Top of Enriched Fuel (in.)	130.0
Containment Drywell Pressure (psia)	16.5
Containment Wetwell Pressure (psia)	14.7
Containment Wetwell Liquid Temperature (°F)	165.0
Maximum Bundle Power (MW_{th})	7.3
Maximum Average Planar Linear Heat Generation Rate (kW/ft)	13.6*
Maximum Linear Heat Generation Rate (kW/ft)	14.4**

---

* Plus Calorimetric and TIP Reading Uncertainties (8.9%)

** Plus Calorimetric and TIP Reading Uncertainties (9.2%)

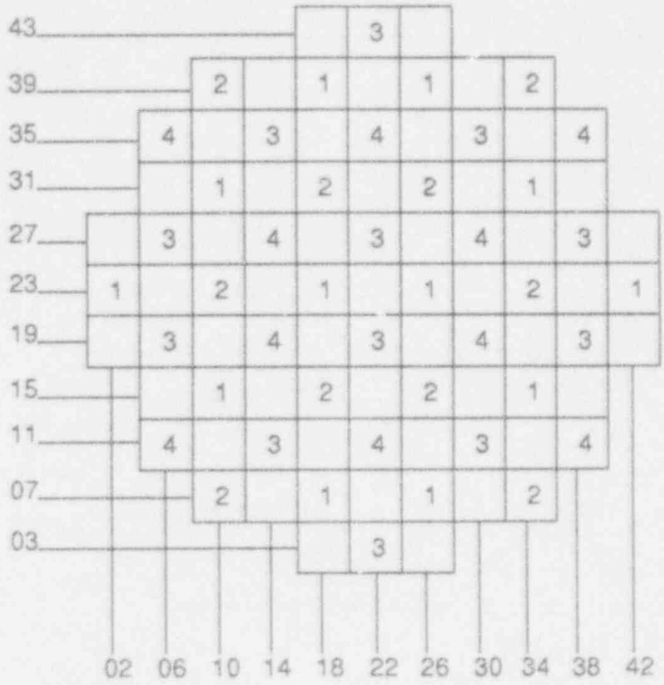

FIGURE 8.1.1

FIRST FOUR ROD ARRAYS PULLED IN THE A SEQUENCES

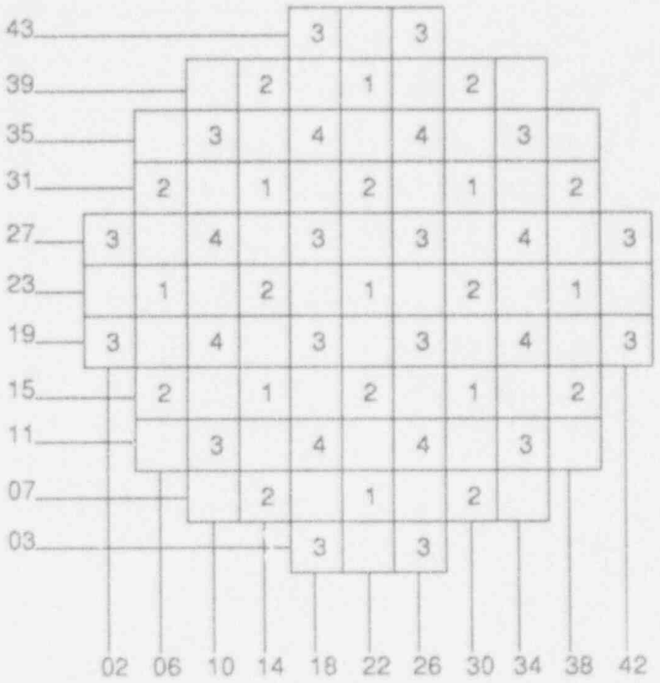

FIGURE 8.1.2

FIRST FOUR ROD ARRAYS PULLED IN THE B SEQUENCES

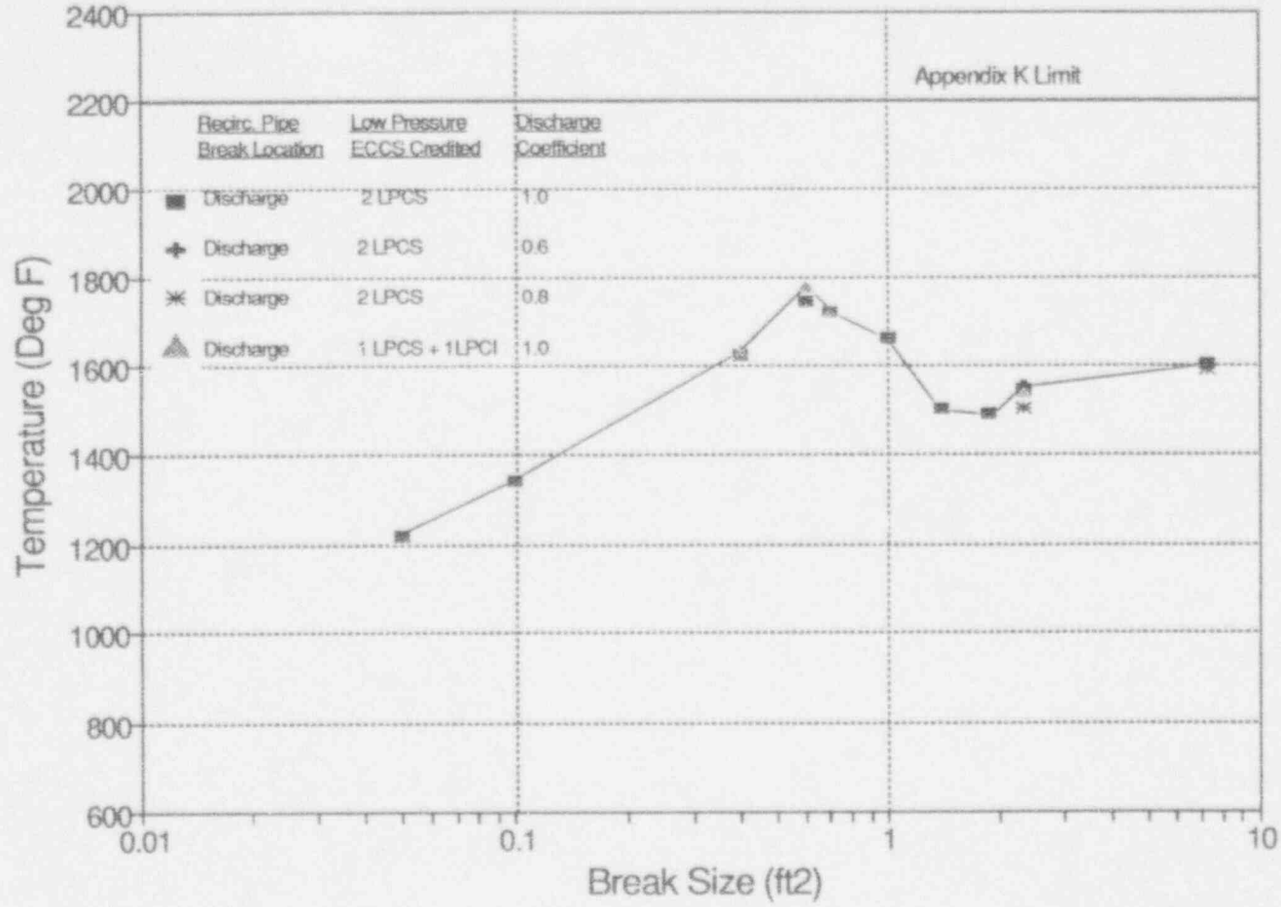

FIGURE 8.2.1

LOCA ANALYSIS RESULTS, PEAK CLADDING TEMPERATURE VERSUS BREAK SIZE

9.0 STARTUP PROGRAM

Following refueling and prior to vessel reassembly, fuel assembly position and orientation will be verified and videotaped by underwater television.

The Vermont Yankee Startup Program will include process computer data checks, shutdown margin demonstration, in-sequence critical measurement, rod scram tests, power distribution comparisons, TIP reproducibility, and TIP symmetry checks. The content of the Startup Test Report will be similar to that sent to the Office of Inspection and Enforcement in the past[39].

REFERENCES

1. J. N. Neyman, Vermont Yankee Cycle 15 Summary Report, YAEC-1850 (June 1992).

2. General Electric Company, General Electric Standard Application for Reactor Fuel (GESTARII), NEDE-24011-P-A-10, GE Company Proprietary, February 1991, as amended.

3. Letter, D. T. Weiss to J. M. Buchheit, "GE9B Bundle Nuclear Design Reports for Reload 14," DTW89168, October 6, 1989.

4. Letter, D. T. Weiss to R. T. Yee, "Fuel Bundle Nuclear Design Reports for Vermont Yankee Reload 16," DTW92194, September 3, 1992.

5. A. S. DiGiovine, J. P. Gorski, and M. A. Tremblay; SIMULATE-3 Validation and Verification; YAEC-1659-A (September 1988).

6. R. A. Woehlke, et al.; MICBURN-3/CASMO-3/TABLES-3/SIMULATE-3 Benchmarking of Vermont Yankee Cycles 9 through 13; YAEC-1683-A (March 1989).

7. B. Y. Hubbard, et al.; End-of-Full-Power-Life Sensitivity Study for the Revised BWR Licensing Methodology; YAEC-1822 (October 1991).

8. VYNPC Letter to USNRC, "Vermont Yankee LOCA Analysis Method: FROSSTEY Fuel Performance Code (FROSSTEY-2)," FVY 87-116 (December 16, 1987).

9. VYNPC Letter to USNRC, "Responses to Request for Additional Information - FROSSTEY-2 Fuel Performance Code," BVY 91-024 (March 6, 1991).

10. VYNPC Letter to USNRC, "FROSSTEY-2 Fuel Performance Code - Vermont Yankee Response to Remaining Concerns," BVY 92-54 (May 15, 1992).

11. USNRC Letter to L. A. Tremblay, SER, "Vermont Yankee Nuclear Power Station, Safety Evaluation of FROSSTEY-2 Computer Code (TAC No. M68216)," NVY 92-178 (September 24, 1992).

12. Appendix A to Operating License DPR-28 Technical Specifications and Bases for Vermont Yankee Nuclear Power Station, Docket No. 50-271.

13. VYNPC Letter to USNRC, "Inverted Control Rod Poison Tubes at Vermont Yankee," WVY 75-51 (May 16, 1975).

14. USNRC Letter to G. C. Andognini, "Change to Bases," (June 6, 1975).

15. A. S. DiGiovine, et al.; CASMO-3 Validation; YAEC-1363-A (April 1988).

16. A. A. F. Ansari, Methods for the Analysis of Boiling Water Reactors: Steady-State Core Flow Distribution Code (FIBWR), YAEC-1234 (December 1980).

17. A. A. F. Ansari, R. R. Gay, and B. J. Gitnick; FIBWR: A Steady-State Core Flow Distribution Code for Boiling Water Reactors - Code Verification and Qualification Report; EPRI NP-1923; Project 1754-1 Final Report, July 1981.

18. USNRC Letter to J. B. Sinclair, SER, "Acceptance for Referencing in Licensing Actions for the Vermont Yankee Plant of Reports: YAEC-1232, YAEC-1238, YAEC-1299P, and YAEC-1234," NVY 82-157 (September 15, 1982).

19. General Electric Company, GEXL-Plus Correlation Application to BWR 2-6 Reactors GE6 through GE9 Fuel, NEDE-31598P, GE Company Proprietary, July 1989.

20. Letter, D. T. Weiss to R. T. Yee, "Mechanical MAPLHGRs for Vermont Yankee Reload 16," DTW93136, June 3, 1993.

21. Letter, D. T. Weiss to R. T. Yee, "Fuel Rod Thermal-Mechanical Performance Limits," DTW92260, November 19, 1992.

22. A. A. F. Ansari and J. T. Cronin, Methods for the Analysis of Boiling Water Reactors: A Systems Transient Analysis Model (RETRAN), YAEC-1233, (April 1981).

23. USNRC Letter to R. L. Smith, SER, "Amendment No. 70 to Facility License No. DPR-28," (November 27, 1981).

24. V. Chandola, M. P. LeFrancois, and J. D. Robichaud; Application of One-Dimensional Kinetics to Boiling Water Reactor Transient Analysis Methods; YAEC-1693-A, Revision 1 (November 1989).

25. Electric Power Research Institute, RETRAN - A Program for One-Dimensional Transient Thermal-Hydraulic Analysis of Complex Fluid Flow Systems, CCM-5, December 1978.

26. USNRC Letter to T. W. Schnatz, SER, "Acceptance for Referencing of Licensing Topical Reports: EPRI CCM-5 and EPRI NP-1850-CCM," (September 4, 1984).

27. A. A. F. Ansari, K. J. Burns, and D. K. Beller; Methods for the Analysis of Boiling Water Reactors: Transient Critical Power Ratio Analysis (RETRAN-TCPYA01); YAEC-1299P (March 1982).

28. J. T. Cronin, Method for Generation of One-Dimensional Kinetics Data for RETRAN-02, YAEC-1694-A (June 1989).

29. General Electric Company; C. J. Paone, et al.; Rod Drop Accident Analysis for Large Boiling Water Reactors; NEDO-10527; March 1972.

30. General Electric Company; R. C. Stirn, et al.; Rod Drop Accident Analysis for Large Boiling Water Reactors Addendum No. 1, Multiple Enrichment Cores with Axial Gadolinium; NEDO-10527, Supplement 1; July 1972.

31. General Electric Company; R. C. Stirn, et al.; Rod Drop Accident Analysis for Large Boiling Water Reactor Addendum No. 2 Exposed Cores; NEDO-10527, Supplement 2; January 1973.

32. General Electric Company, C. J. Paine, Banked Position Withdrawal Sequence, NEDO-21231, January 1977.

33. General Electric Company, D. Radcliffe and R. E. Bates, Reduced Notch Worth Procedure, SIL-316, November 1979.

34. M. A. Sironen, Vermont Yankee Cycle 14 Core Performance Analysis Report, YAEC-1706 (October 1988).

35. L. Schor, et al.; Vermont Yankee Loss-of-Coolant Accident Analysis; YAEC-1772 (June 1993).

36. USNRC Letter to L. A. Tremblay, SER, "Safety Evaluation for Vermont Yankee Nuclear Power Station RELAP5YA LOCA Analysis Methodology (TAC No. M74595)," NVY 92-192 (October 21, 1992).

37. USNRC Letter to R. W. Capstick, SER, "Approval of Use of Thermal-Hydraulic Code RELAP5YA (TAC No. 60193)," NVY 87-136 (August 25, 1987).

38. Vermont Yankee Nuclear Power Station Final Safety Analysis Report, December 1991.

39. Letter from L. A. Tremblay to USNRC, "Cycle 16 Startup Test Report," BVY 92-77 (July 1, 1992).

APPENDIX A

CALCULATED OPERATING LIMITS

The MCPR operating limits for the Reload Cycle are calculated by adding the calculated ΔCPR to the FCISL. This is done for each of the analyses in Section 7.0 at each of the exposure statepoints. For an exposure interval between statepoints, the highest MCPR limit at either end is assumed to apply to the whole interval.

Table A.1 provides the highest calculated MCPR limits for the Reload Cycle for each of the exposure intervals for the various scram speeds and for the various rod block lines. These MCPR operating limits are valid for operation of the Reload Cycle at full power up to 10760 MWd/St and for operation during coastdown beyond EOFPL.

Tables A.2 through A.5 provide the maximum calculated MAPLHGR limits for all the fuel types in the Reload Cycle. These values are bounding for all the lattice zones in each fuel type.

TABLE A.1

VERMONT YANKEE NUCLEAR POWER STATION

CYCLE 17 MCPR OPERATING LIMITS

Value of "N" in RBM Equation(1)	Average Control Rod Scram Time	Cycle Exposure Range	MCPR Operating Limit(2),(3)
42%	Equal to or better than L.C.O. 3.3.C.1.1	0 to 4000 MWd/St	1.42
		4000 to 10760 MWd/St	1.34
	Equal to or better than L.C.O. 3.3.C.1.2	0 to 4000 MWd/St	1.42
		4000 to 10760 MWd/St	1.34
41%	Equal to or better than L.C.O. 3.3.C.1.1	0 to 4000 MWd/St	1.42
		4000 to 5500 MWd/St	1.34
		5500 to 9170 MWd/St	1.30
		9170 to 10760 MWd/St	1.32
	Equal to or better than L.C.O. 3.3.C.1.2	0 to 4000 MWd/St	1.42
		4000 to 5500 MWd/St	1.34
		5500 to 9170 MWd/St	1.30
		9170 to 10760 MWd/St	1.34
≤ 40%	Equal to or better than L.C.O. 3.3.C.1.1	0 to 4000 MWd/St	1.42
		4000 to 5500 MWd/St	1.34
		5500 to 6500 MWd/St	1.28
		6500 to 8170 MWd/St	1.25
		8170 to 9170 MWd/St	1.27
		9170 to 10760 MWd/St	1.32
	Equal to or better than L.C.O. 3.3.C.1.2	0 to 4000 MWd/St	1.42
		4000 to 5500 MWd/St	1.34
		5500 to 6500 MWd/St	1.28
		6500 to 8170 MWd/St	1.25
		8170 to 9170 MWd/St	1.30
		9170 to 10760 MWd/St	1.34

(1) The Rod Block Monitor (RBM) trip setpoints are determined by the equation shown in Table 3.2.5 of the Technical Specifications.

(2) The current analysis for the MCPR operating limits does not include the 7X7, 8X8, 8X8R or P8X8R fuel types. On this basis, if any of these fuel types are to be reinserted, they will be evaluated in accordance with 10CFR50.59 to ensure that the above limits are bounding for these fuel types.

(3) MCPR operating limits should be increased by 0.01 for the single loop operation.

TABLE A.2

MAPLHGR VERSUS AVERAGE PLANAR EXPOSURE FOR BP8DWB311-10GZ

Plant: Vermont Yankee

Fuel Type: BP8DWB311-10GZ

Average Planar Exposure	MAPLHGR Limits (kW/ft)	
(MWd/St)	Two-Loop Operation	Single-Loop Operation*
0.00	10.93	9.07
200.00	11.00	9.13
1,000.00	11.13	9.24
2,000.00	11.32	9.40
3,000.00	11.52	9.56
4,000.00	11.64	9.66
5,000.00	11.77	9.77
6,000.00	11.92	9.89
7,000.00	12.11	10.05
8,000.00	12.34	10.24
9,000.00	12.59	10.45
10,000.00	12.83	10.65
12,500.00	13.00	10.79
15,000.00	12.81	10.63
20,000.00	12.24	10.16
25,000.00	11.55	9.59
35,000.00	10.24	8.50
45,000.00	8.76	7.27
51,299.00	5.87	4.87

* MAPLHGR limits for single-loop operation are obtained by multiplying the two-loop operation MAPLHGR limits by 0.83.

TABLE A.3

MAPLHGR VERSUS AVERAGE PLANAR EXPOSURE FOR BP8DWB311-11GZ

Plant: Vermont Yankee

Fuel Type: BP8DWB311-11GZ

Average Planar Exposure	MAPLHGR Limits (kW/ft)	
(MWd/St)	Two-Loop Operation	Single-Loop Operation*
0.00	10.93	9.07
200.00	11.00	9.13
1,000.00	11.13	9.24
2,000.00	11.32	9.40
3,000.00	11.52	9.56
4,000.00	11.64	9.66
5,000.00	11.77	9.77
6,000.00	11.92	9.89
7,000.00	12.11	10.05
8,000.00	12.34	10.24
9,000.00	12.59	10.45
10,000.00	12.83	10.65
12,500.00	13.00	10.79
15,000.00	12.81	10.63
20,000.00	12.24	10.16
25,000.00	11.55	9.59
35,000.00	10.24	8.50
45,000.00	8.76	7.27
51,466.00	5.83	4.84

* MAPLHGR limits for single-loop operation are obtained by multiplying the two-loop operation MAPLHGR limits by 0.83.

TABLE A.4

MAPLHGR VERSUS AVERAGE PLANAR EXPOSURE FOR BP8DWB335-10GZ

Plant: Vermont Yankee

Fuel Type: BP8DWB335-10GZ

Average Planar Exposure	MAPLHGR Limits (kW/ft)	
(MWd/St)	Two-Loop Operation	Single-Loop Operation*
0.00	11.29	9.37
200.00	11.34	9.41
1,000.00	11.48	9.53
2,000.00	11.69	9.70
3,000.00	11.92	9.89
4,000.00	12.17	10.10
5,000.00	12.43	10.32
6,000.00	12.68	10.52
7,000.00	12.87	10.68
8,000.00	13.06	10.84
9,000.00	13.24	10.99
10,000.00	13.35	11.08
12,500.00	13.20	10.96
15,000.00	13.01	10.80
20,000.00	12.27	10.18
25,000.00	11.43	9.49
35,000.00	9.88	8.20
45,000.00	8.38	6.96
50,593.00	5.65	4.69

* MAPLHGR limits for single-loop operation are obtained by multiplying the two-loop operation MAPLHGR limits by 0.83.

TABLE A.5

MAPLHGR VERSUS AVERAGE PLANAR EXPOSURE FOR BP8DWB335-11GZ

Plant: Vermont Yankee

Fuel Type: BP8DWB335-11GZ

Average Planar Exposure	MAPLHGR Limits (kW/ft)	
(MWd/St)	Two-Loop Operation	Single-Loop Operation*
0.00	11.28	9.36
200.00	11.33	9.40
1,000.00	11.43	9.49
2,000.00	11.60	9.63
3,000.00	11.80	9.79
4,000.00	12.04	9.99
5,000.00	12.30	10.21
6,000.00	12.53	10.40
7,000.00	12.73	10.57
8,000.00	12.94	10 4
9,000.00	13.13	10.90
10,000.00	13.29	11.03
12,500.00	13.20	10.96
15,000.00	12.99	10.78
20,000.00	12.27	10.18
25,000.00	11.43	9.49
35,000.00	9.88	8.20
45,000.00	8.38	6.96
50,593.00	5.65	4.69

* MAPLHGR limits for single-loop operation are obtained by multiplying the two-loop operation MAPLHGR limits by 0.83.